

# Self-complementary nickel halides enable multifaceted comparisons of intermolecular halogen bonds: fluoride ligands vs other halides

Vargini Thangavadivale, Pedro Aguiar, Naseralla A. Jasim, Sarah J. Pike, Dan A. Smith, Adrian C. Whitwood, Lee Brammer and Robin N. Perutz

## Supporting Information

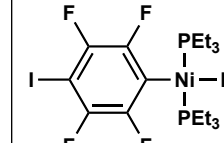
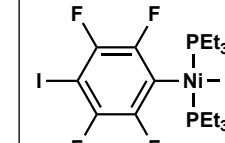
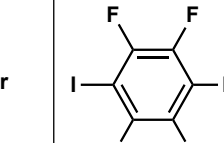
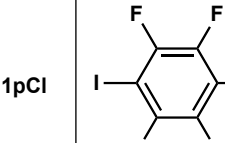
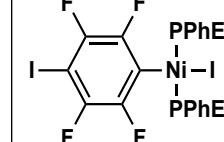
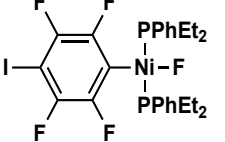
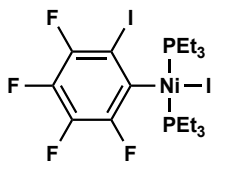
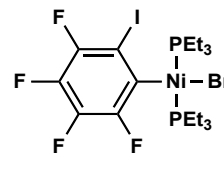
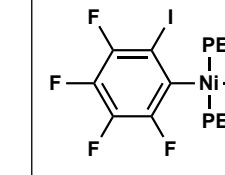
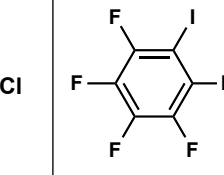
### Table of Contents

Table S1	Complexes prepared to study the halogen bonding interactions in the solid state.	S4
Figure S1	$^{31}\text{P}\{\text{H}\}$ -NMR (202 MHz) spectrum of <b>1pF</b> in $\text{C}_6\text{D}_6$ .	S5
Figure S2	$^{19}\text{F}$ -NMR (470 MHz) spectrum of <b>1pF</b> in $\text{C}_6\text{D}_6$ .	S5
Figure S3	$^{19}\text{F}$ -NMR (470 MHz) spectrum of <b>1pF</b> in $\text{C}_6\text{D}_6$ .	S5
Figure S4.	LIFDI mass spectrum showing the isotopic pattern of <b>1pF</b> .	S6
Figure S5	Molecular structure of <b>1pF</b> ..	S6
Table S2	Selected bond lengths ( $\text{\AA}$ ) and angles ( $^\circ$ ) of <b>1pF</b>	S7
Figure S6	Molecular structure of <b>1pCl</b> ..	S7
Table S3	Selected bond lengths ( $\text{\AA}$ ) and angles ( $^\circ$ ) of <b>1pCl</b> .	S8
Figure S7.	Molecular structure of <b>1pBr</b> .	S8
Table S4	Selected bond lengths ( $\text{\AA}$ ) and angles ( $^\circ$ ) of <b>1pBr</b> .	S9
Figure S8	$^{31}\text{P}\{\text{H}\}$ -NMR (202 MHz) spectrum of crude <b>1pI</b> in $\text{C}_6\text{D}_6$ .	S9
Figure S9	$^{19}\text{F}$ -NMR (470 MHz) spectrum of crude <b>1pI</b> in $\text{C}_6\text{D}_6$ .	S10
Figure S10	$^{31}\text{P}\{\text{H}\}$ -NMR (202 MHz) spectrum of <b>1pI</b> in $\text{C}_6\text{D}_6$ after purification	S10
Table S5	Selected bond lengths ( $\text{\AA}$ ) and angles ( $^\circ$ ) of <b>1pI</b> .	S11
Figure S11.	Molecular structure of <b>1pI</b>	S11
Table S6.	Crystal data for complexes <b>1pF</b> , <b>1pCl</b> <b>1pBr</b> and <b>1pI</b> ,	S12
	Refinement of crystal structure for <b>1pF</b> .	S13
	Dinuclear products: $[\text{NiX}(\text{PEt}_3)_2]_2(\mu\text{-2,3,5,6-C}_6\text{F}_4)$ ( $\text{X} = \text{Br}, \text{I}$ ).	S13
Figure S12	LIFDI mass spectrum showing the isotopic pattern of <i>trans</i> - $[\text{NiI}(\text{PEt}_3)_2]_2(\mu\text{-2,3,5,6-C}_6\text{F}_4)$ .	S14
Figure S13	Molecular structure of $[\text{NiBr}(\text{PEt}_3)_2]_2(\mu\text{-2,3,5,6-C}_6\text{F}_4)$ showing	S14

	two independent molecules in cell.	
Table S7.	Selected bond lengths ( $\text{\AA}$ ) and angles ( $^\circ$ ) of $[\text{Ni}(\text{Br})(\text{PEt}_3)_2]_2(\mu\text{-2,3,5,6-C}_6\text{F}_4)$	S15
Figure S14.	$^{31}\text{P}\{^1\text{H}\}$ -NMR (202 MHz) spectrum of <b>2pF</b> in $\text{C}_6\text{D}_6$ .	S15
Figure S15.	$^{19}\text{F}$ -NMR (470 MHz) spectrum of <b>2pF</b> in $\text{C}_6\text{D}_6$ .	S15
Figure S16	$^{31}\text{P}\{^1\text{H}\}$ -NMR (202 MHz) spectrum of <b>2pI</b> in $\text{C}_6\text{D}_6$ .	S16
Figure S17	$^{19}\text{F}$ -NMR (470 MHz) spectrum of <b>2pI</b> in $\text{C}_6\text{D}_6$	S16
Figure S18	Molecular structure of <b>2pI</b> .	S17
Table S8	Selected bond lengths ( $\text{\AA}$ ) and angles ( $^\circ$ ) of <b>2pI</b> .	S18
Figure S19.	$^{31}\text{P}\{^1\text{H}\}$ -NMR (202 MHz) spectrum of <b>1oF</b> in $\text{C}_6\text{D}_6$	S19
Figure S20.	$^{19}\text{F}$ -NMR (470 MHz) spectrum of <b>1oF</b> in $\text{C}_6\text{D}_6$ in high field region.	S19
Figure S21.	$^{19}\text{F}$ -NMR (470 MHz) spectrum of <b>1oF</b> in $\text{C}_6\text{D}_6$ in fluoroaromatic region: above $^{19}\text{F}$ NMR spectrum, below F-F COSY spectrum	S20
Figure S22.	LIFDI mass spectrum of <b>1oF</b> . Above full spectrum. Below expansion and simulation.	S21
Figure S23	Molecular structure of <b>1oF</b> .	S22
Table S9	Selected bond lengths ( $\text{\AA}$ ) and angles ( $^\circ$ ) of <b>1oF</b> .	S22
Figure S24.	$^1\text{H}$ NMR spectrum of <b>1oCl</b> in $\text{C}_6\text{D}_6$	S23
Figure S25.	$^{31}\text{P}\{^1\text{H}\}$ NMR spectrum (above) of <b>1oCl</b> in $\text{C}_6\text{D}_6$ and $^{31}\text{P}$ - $^1\text{H}$ correlation (below).	S24
Figure S26.	$^{19}\text{F}$ NMR spectrum of <b>1oCl</b> in $\text{C}_6\text{D}_6$ . Above $^{19}\text{F}$ NMR, below $^{19}\text{F}$ - $^{19}\text{F}$ COSY	S25
Figure S27	LIFDI mass spectrum of <b>1oCl</b> . Above full spectrum. Below expansion and simulation.	S26
Figure S28.	Molecular structure of <b>1oCl</b> .	S27
Table S10.	Selected bond lengths ( $\text{\AA}$ ) and angles ( $^\circ$ ) of <b>1oCl</b> .	S27
Figure S29.	$^1\text{H}$ NMR spectrum of <b>1oBr</b> in $\text{C}_6\text{D}_6$ .	S28
Figure S30.	$^{31}\text{P}\{^1\text{H}\}$ NMR spectrum (above) of <b>1oBr</b> in $\text{C}_6\text{D}_6$ and $^{31}\text{P}$ - $^1\text{H}$ correlation (below)	S29
Figure S31.	$^{19}\text{F}$ NMR spectrum of <b>1oBr</b> in $\text{C}_6\text{D}_6$ . Above $^{19}\text{F}$ NMR, below $^{19}\text{F}$ - $^{19}\text{F}$ COSY	S30
Figure S32.	LIFDI mass spectrum of <b>1oBr</b> . Above full spectrum. Below expansion and simulation.	S31
Figure S33.	Above $^1\text{H}$ NMR spectrum of <b>1oI</b> in $\text{C}_6\text{D}_6$ . Below $^1\text{H}\{^{31}\text{P}\}$ NMR	S32

	of <b>1oI</b> .	
Figure S34.	$^1\text{H}$ - $^{31}\text{P}$ HMQC of <b>1oI</b>	S33
Figure S35	$^{31}\text{P}\{^1\text{H}\}$ -NMR (202 MHz) spectrum of <b>1oI</b> in $\text{C}_6\text{D}_6$	S33
Figure S36.	Above: $^{19}\text{F}$ -NMR spectrum (470 MHz) spectrum of <b>1oI</b> in $\text{C}_6\text{D}_6$ . Below: $^{19}\text{F}$ - $^{19}\text{F}$ COSY spectrum	S34
Figure S37.	LIFDI mass spectrum of <b>1oI</b> . Above full spectrum. Below expansion and simulation.	S35
Figure S38.	Molecular structure of <b>1oI</b> . Above: <b>1oI</b> ( $\alpha$ ). Middle: <b>1oI</b> ( $\beta$ ) Below: <b>1oI</b> ( $\gamma$ )	S36
Table S11	Selected bond lengths ( $\text{\AA}$ ) and angles ( $^\circ$ ) of <b>1oI</b> ( $\alpha$ )	S37
Table S12.	Crystal data for complexes <b>2pI</b> , <b>1oF</b> , <b>1oCl</b> and <b>1oI</b>	S38
	Refinement details for <b>1oX</b>	S40
Figure S39.	$^{19}\text{F}$ -NMR (470 MHz) spectrum of the sample containing $\text{Ni}(\text{PEt}_3)_2(\text{C}_6\text{F}_4)$ .	S41
Figure S40.	Molecular structure of $\text{Ni}(\text{PEt}_3)_2(\eta^2\text{-C}_6\text{F}_4)$ .	S41
Table S13.	Selected bond lengths ( $\text{\AA}$ ) and angles ( $^\circ$ ) of $\text{Ni}(\text{PEt}_3)_2(\text{C}_6\text{F}_4)$	S42
Table S14	Crystal data for $\text{Ni}(\text{PEt}_3)_2(\text{C}_6\text{F}_4)$ and $[\text{Ni}(\text{Br})(\text{PEt}_3)_2]_2(\mu\text{-2,3,5,6-C}_6\text{F}_4)$	S43
	Crystallographic Method for $[\text{Ni}(\text{Br})(\text{PEt}_3)_2]_2(\mu\text{-2,3,5,6-C}_6\text{F}_4)$	S44
Figure S41.	Above: overlay of structures of <b>1pF</b> at 200 K (red) and 240 K (green). Below: Diagram showing halogen-bonded chain in structure of <b>1pF</b> at 240 K.	S45
Table S15	Crystal data and structure refinement for <b>1pF</b> at variable temperatures.	S46
Figure S42.	$^{19}\text{F}$ -MAS SSNMR spectrum of complex <b>1oF</b> .	S47
Figure S43	$^{19}\text{F}$ -MAS SSNMR spectrum of <b>3F</b> <i>trans</i> - $[\text{NiF}(\text{C}_6\text{F}_5)(\text{PEt}_3)_2]$ .	S47
Figure S44.	$^{31}\text{P}\{^1\text{H}\}$ CPMAS spectrum of <b>1pF</b> .	S48
	Gaussian Ref:	S48
Table S16.	Calculated Geometry for <i>trans</i> - $[\text{NiF}(2,3,5,6\text{-C}_6\text{F}_4\text{I})(\text{PMMe}_3)_2]$	S49
Table S17.	Calculated Geometry for <i>trans</i> - $[\text{NiF}(2,3,5,6\text{-C}_6\text{F}_4\text{I})(\text{PMMe}_3)_2 + (2,3,5,6\text{-C}_6\text{F}_4\text{I})]$	S50

**Table S1** Complexes prepared to study the halogen bonding interactions in the solid state.

		<b>Iodide</b>	<b>Bromide</b>	<b>Chloride</b>	<b>Fluoride</b>
(1,4-C <sub>6</sub> F <sub>4</sub> I <sub>2</sub> )	Triethyl phosphines	 1pl	 1pBr	 1pCl	 1pF
	Diethylphenyl phosphine	 2pl			 2pF
(1,2-C <sub>6</sub> F <sub>4</sub> I <sub>2</sub> )	Triethyl phosphine	 1oI	 1oBr	 1oCl	 1oF

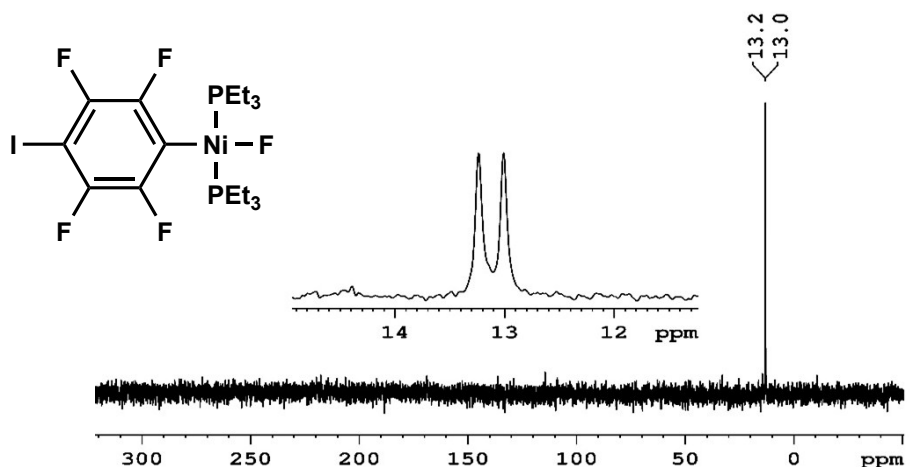


**Figure S1**  $^{31}\text{P}\{\text{H}\}$ -NMR (202 MHz) spectrum of **1pF** in  $\text{C}_6\text{D}_6$ .

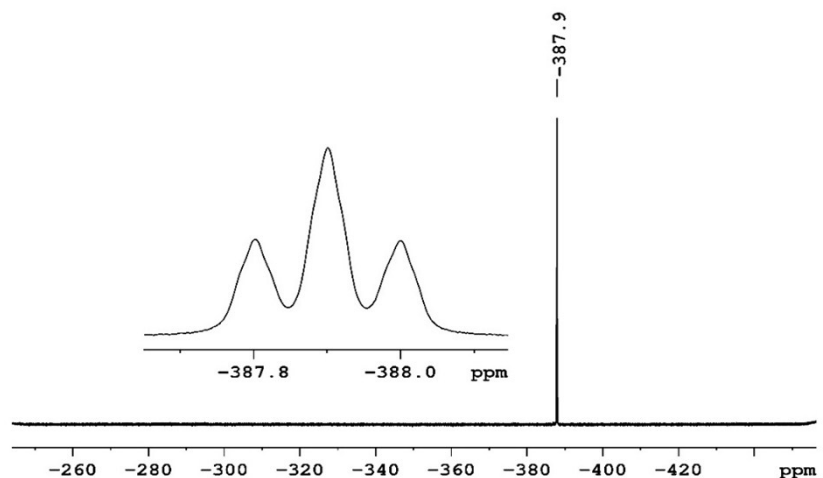


**Figure S2**  $^{19}\text{F}$ -NMR (470 MHz) spectrum of **1pF** in  $\text{C}_6\text{D}_6$ .

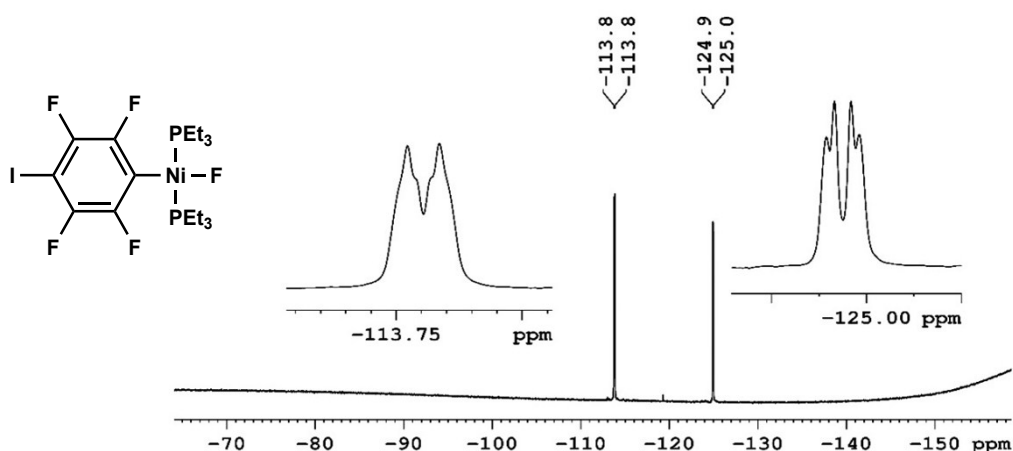


**Figure S3**  $^{19}\text{F}$ -NMR (470 MHz) spectrum of **1pF** in  $\text{C}_6\text{D}_6$ .

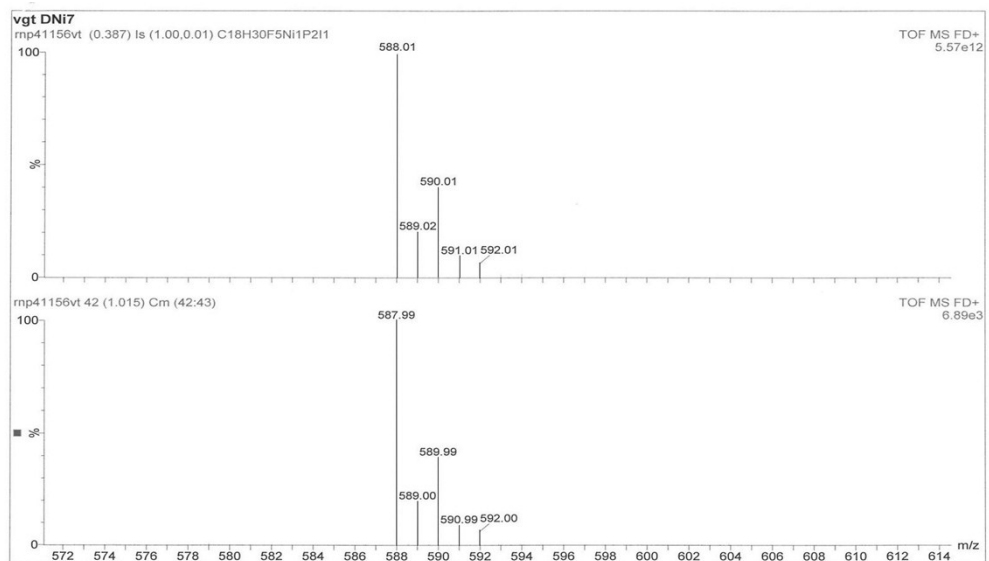


**Figure S4.** LIFDI mass spectrum showing the isotopic pattern of **1pF**.

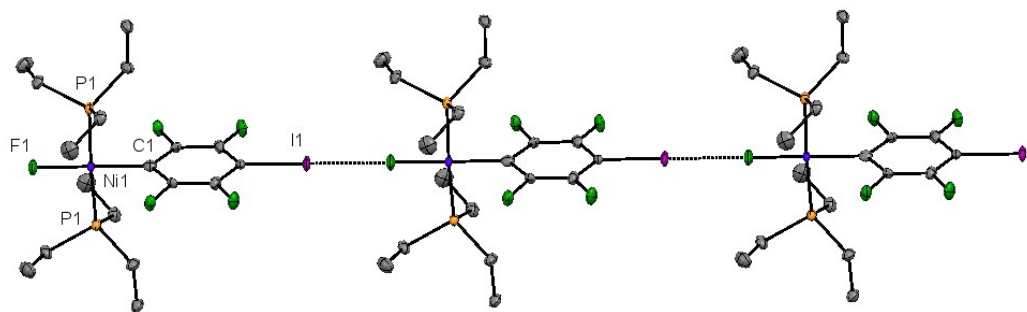


**Figure S5** Molecular structure of **1pF**. Displacement ellipsoids at 50% probability level.

Hydrogen atoms are omitted for clarity.

**Table S2** Selected bond lengths ( $\text{\AA}$ ) and angles ( $^\circ$ ) of **1pF**.

I1-C1	2.103(7)	C5-F1	1.34(1)
Ni1-P1	2.209(2)	C7-F6	1.35(1)
Ni1-F2	1.827(5)	P1-C5	1.830(7)
Ni1-C1	1.852(9)	C3-C2-F2	117.0(6)
F3-C6	1.362(9)	P1-Ni1-F1	91.5
C5-C6	1.571(7)	P1-Ni1-C1	88.5

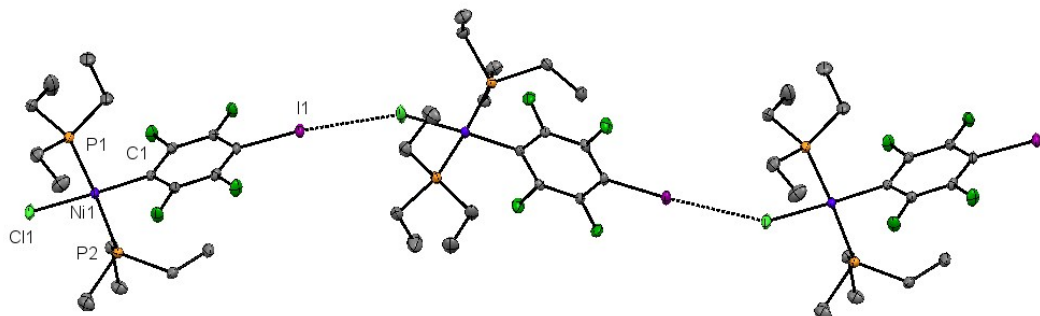


**Figure S6** Molecular structure of **1pCl**. Displacement ellipsoids at 50% probability level and hydrogen atoms are omitted for clarity..

**Table S3** Selected bond lengths ( $\text{\AA}$ ) and angles ( $^\circ$ ) of **1pCl**.

C1-C2	1.382(2)	Cl1-Ni1	2.2037(5)
C1-Ni1	1.881(2)	Ni1-P1	2.2086(5)
C2-C3	1.381(2)	C7-C8	1.515(3)
C2-F2	1.361(2)	C4-I1...Cl1	167.09(5)
C3-C4	1.385(2)	I1...Cl1-Ni1	146.8(2)
C3-F3	1.350(2)	C7-P1-C11	103.12(9)
C4-I1	2.082(2)	C8-C7-P1	113.9(1)
C7-P1	1.825(2)	Cl1-Ni1-C1	175.83(5)

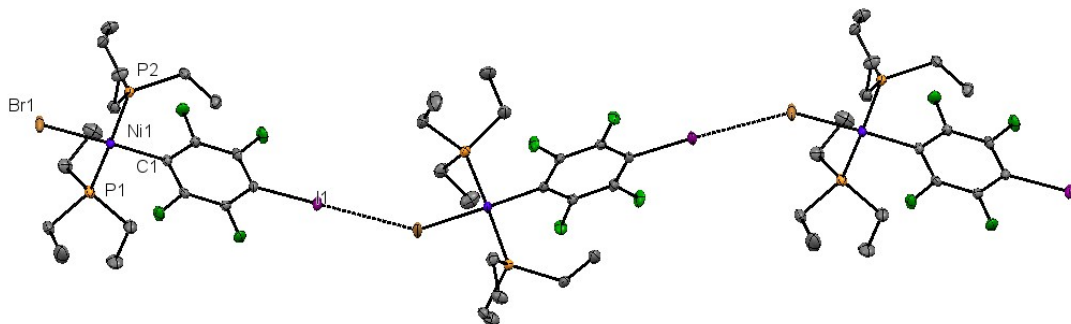


**Figure S7.** Molecular structure of **1pBr**. Displacement ellipsoids at 50% probability level. Hydrogen atoms are omitted for clarity.

**Table S4** Selected bond lengths ( $\text{\AA}$ ) and angles ( $^\circ$ ) of **1pBr**.

I1-C4	2.082(2)	C3-C4	1.372(3)
Ni1-Br1	2.3384(3)	C2-C3	1.384(3)
Ni1-P2	2.2176(6)	C13-C14	1.512(4)
Ni1-C1	1.881(2)	Br1-Ni1-C1	176.61(6)
F1-C6	1.359(2)	C4-I2…Br1	167.6(6)
F2-C5	1.349(2)	I2…Br1-Ni1	143.3(1)
C1-C2	1.382(3)	C13-P1-C17	103.3(1)

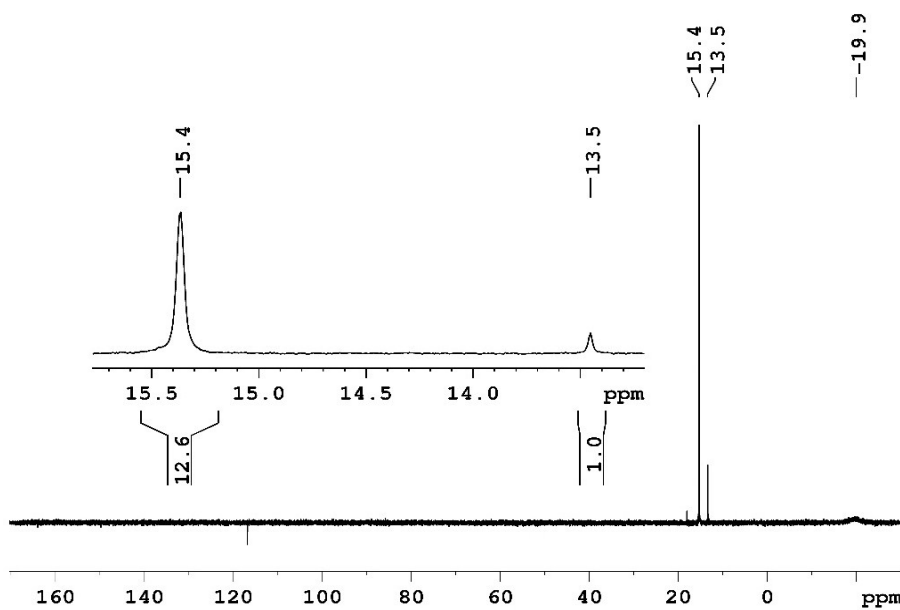


**Figure S8**  $^{31}\text{P}\{^1\text{H}\}$ -NMR (202 MHz) spectrum of crude **1pI** in  $\text{C}_6\text{D}_6$ .

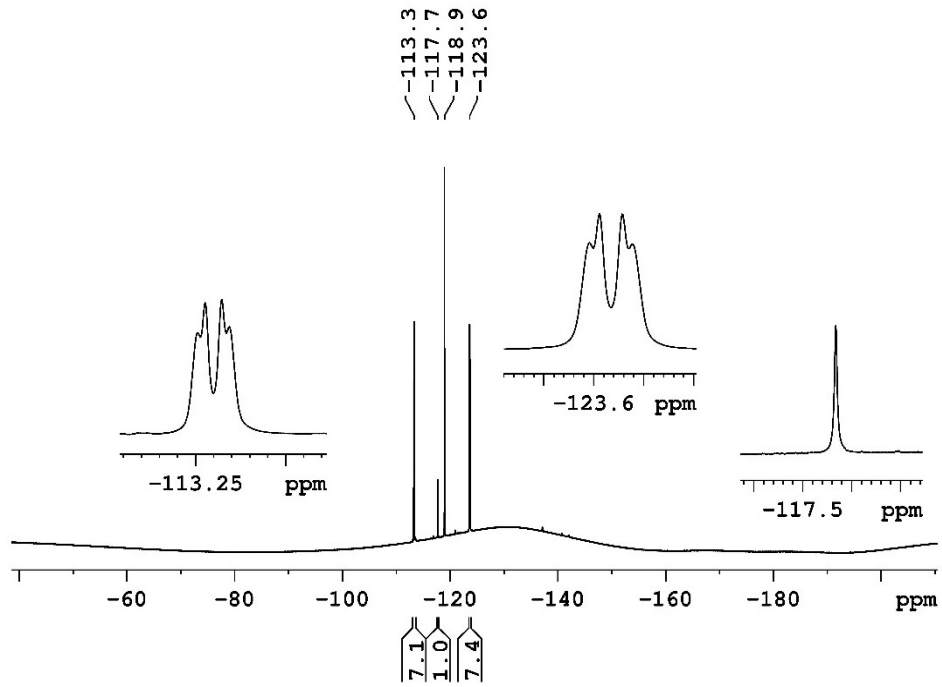


**Figure S9**  $^{19}\text{F}$ -NMR (470 MHz) spectrum of crude **1pl** in  $\text{C}_6\text{D}_6$ .

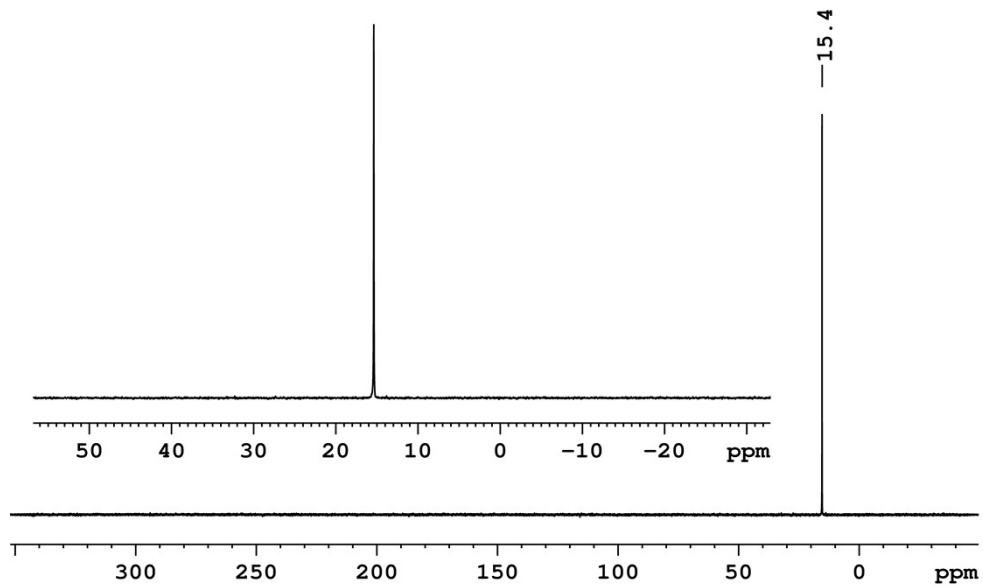


**Figure S10**  $^{31}\text{P}\{\text{H}\}$ -NMR (202 MHz) spectrum of **1pl** in  $\text{C}_6\text{D}_6$  after purification

**Table S5** Selected bond lengths (Å) and angles (°) of **1pl**.

I2-C4	2.093(6)	C6-C1	1.376(9)
Ni1-P1	2.224(2)	F1-C2	1.341(7)
Ni1-I1	2.5221(9)	F2-C3	1.350(7)
Ni1-C1	1.877(6)	C4-I2…I1	168.0(2)
P2-C17	1.838(7)	I2…I1-Ni1	139.2(2)
C5-C6	1.381(8)	C15-P2-C13	103.3(3)
C5-C4	1.394(9)	I1-Ni1-C1	178.3(2)
C13-C14	1.51(1)	P1-Ni1-P2	178.33(7)

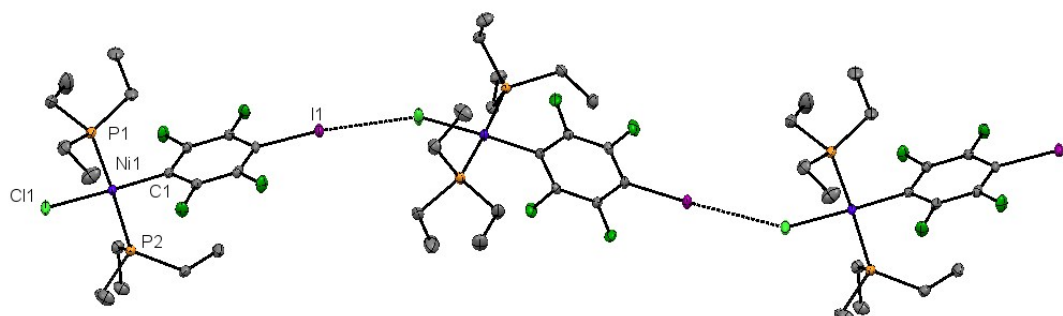


**Figure S11.** Molecular structure of **1pl** Thermal ellipsoids set at 50% level. Hydrogen atoms are omitted for clarity.

**Table S6.** Crystal data for complexes **1pF**, **1pCl** **1pBr** and **1pl**.

	<b>1pF</b>	<b>1pCl</b>	<b>1pBr</b>	<b>1pl</b>
	1825439	1825443	1825444	1825445
Formula	C <sub>18</sub> H <sub>30</sub> F <sub>5</sub> INiP <sub>2</sub>	C <sub>18</sub> H <sub>30</sub> ClF <sub>4</sub> INiP <sub>2</sub>	C <sub>18</sub> H <sub>30</sub> BrF <sub>4</sub> INiP <sub>2</sub>	C <sub>18</sub> H <sub>30</sub> F <sub>4</sub> I <sub>2</sub> NiP <sub>2</sub>
M	588.97	605.42	649.88	696.87
a/ Å	7.8675(5)	9.95341(11)	9.95422(18)	9.9032(3)
b/ Å	11.3291(3)	16.0611(2)	16.0712(3)	16.1922(6)
c/ Å	12.9347(6)	15.04577(13)	15.0877(3)	15.2884(7)
Vol/ Å <sup>3</sup>	1149.51(10)	2387.31(4)	2401.41(8)	2445.85(17)
T/ K	110	110	110	110
α /°	90	90.00	90.00	90.00
β /°	94.392(5)	97.0034(9)	95.7803(19)	93.913(4)
γ /°	90	90.00	90.00	90.00
Space gp	I2	P2 <sub>1</sub> /c	P2 <sub>1</sub> /c	P2 <sub>1</sub> /c
Z	2	4	4	4
μ (Mo Kα mm <sup>-1</sup> )	0.7107	0.7107	0.7107	0.7107
Reflections collected	5693	18822	22833	12397
Ind reflections	2011	7680	7765	6325
R <sub>(int)</sub>	0.0382	0.0244	0.0346	0.0326
Final R [I≥2σ (I)]	R <sub>1</sub> = 0.0255	R <sub>1</sub> = 0.0254	R <sub>1</sub> = 0.0277	R <sub>1</sub> = 0.0578
	wR <sub>2</sub> = 0.0592	wR <sub>2</sub> = 0.0497	wR <sub>2</sub> = 0.0543	wR <sub>2</sub> = 0.101
Final R [all data]	R <sub>1</sub> = 0.0255	R <sub>1</sub> = 0.0254	R <sub>1</sub> = 0.0277	R <sub>1</sub> = 0.0816
	wR <sub>2</sub> = 0.0592	wR <sub>2</sub> = 0.0497	wR <sub>2</sub> = 0.0543	wR <sub>2</sub> = 0.109

Flack parameter	0.087(15)	n/a	n/a	n/a
-----------------	-----------	-----	-----	-----

**Refinement of crystal structure for 1pF.** The crystal of **1pF** exhibited multi-crystal (non-merohedral) twinning which was modelled using CrysAlisPro. The twinning may have resulted from slight cracking of the crystal on cooling. Inclusion of both components of the twin gave a poorer fit than just using a single component from the twin analysis, as judged by the  $R$ ,  $wR2$ ,  $GOOF$  indices and the anisotropic displacement ellipsoid shapes. Therefore, only data from the major component were used, and reflections showing significant overlap with those of the minor component were omitted. The molecule is situated on a two-fold rotation axis parallel to the  $b$ -axis which passes along the Ni–F bond and bisects the phenyl ring. The ADP of atom F1 was restrained to be approximately isotropic.

**Dinuclear products:**  $[\text{trans-NiX}(\text{PEt}_3)_2]_2(\mu\text{-2,3,5,6-C}_6\text{F}_4)$  ( $\text{X} = \text{Br, I}$ ). The product arising from the oxidative addition of both iodine atoms on  $1,4\text{-C}_6\text{F}_4\text{I}_2$ ,  $[\text{trans-NiI}(\text{PEt}_3)_2]_2(\mu\text{-2,3,5,6-C}_6\text{F}_4)$ , when reacted with tetramethylammonium bromide gave rise to  $[\text{trans-NiBr}(\text{PEt}_3)_2]_2(\mu\text{-2,3,5,6-C}_6\text{F}_4)$ , the identity of which was confirmed by X-ray crystallographic studies. Single crystals of the complex were grown from hexane. The structure of  $[\text{trans-NiBr}(\text{PEt}_3)_2]_2(\mu\text{-2,3,5,6-C}_6\text{F}_4)$ , showed two nickel centres bound to the fluoroaromatic ring,  $\text{C}_6\text{F}_4$ , para to each other. Two triethyl phosphine groups *trans* to each other and a bromide completed the square-planar geometry around the metal centres. The plane of the metal coordination centre and the plane of the aromatic ring were near perpendicular to each other ( $88.2^\circ$ ). Selected bond lengths and angles are given in Table S7 and crystal data in Table S14.

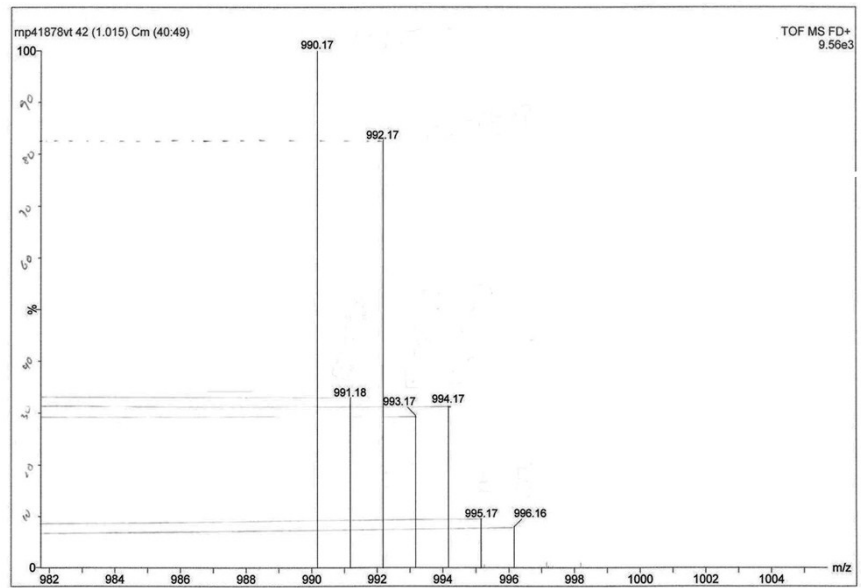


**Figure S11** LIFDI mass spectrum showing the isotopic pattern of  $[trans\text{-}Ni(PEt_3)_2]_2(\mu\text{-}2,3,5,6\text{-C}_6F_4)$ .

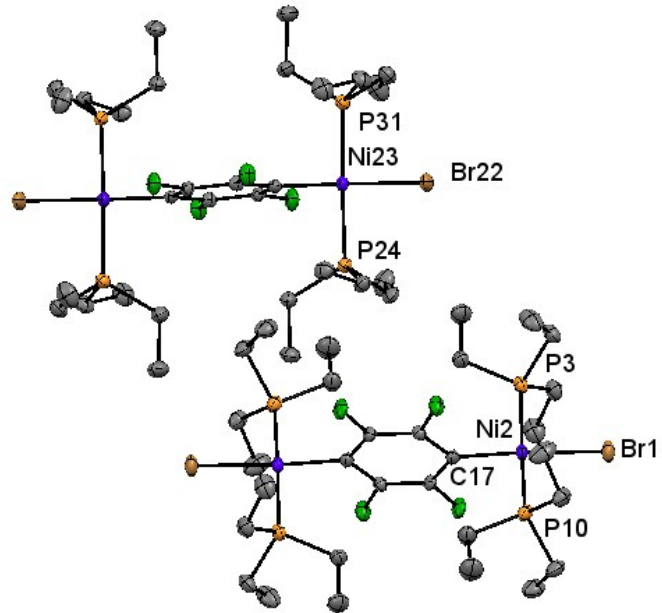


**Figure S13** Molecular structure of  $[trans\text{-}NiBr(PEt_3)_2]_2(\mu\text{-}2,3,5,6\text{-C}_6F_4)$  showing two independent molecules in cell. Displacement ellipsoids at 50% probability level and hydrogen atoms are omitted for clarity.

**Table S7.** Selected bond lengths ( $\text{\AA}$ ) and angles ( $^\circ$ ) of  $[\text{trans-NiBr}(\text{PEt}_3)_2]_2(\mu\text{-2,3,5,6-C}_6\text{F}_4)$ .

Br1-Ni2	2.3547(3)	C18-F21	1.370(3)
Ni2-P3	2.2165(7)	Br1-Ni2-C17	172.87(7)
Ni2-P10	2.2147(7)	P3-Ni2-P10	172.36(3)
Ni2-C17	1.898(2)	Ni2-C17-C19	122.5(2)
P3-C4	1.829(3)	F21-C18-C17	118.8(2)
C17-C18	1.392(3)	P10-Ni2-C17	92.21(7)

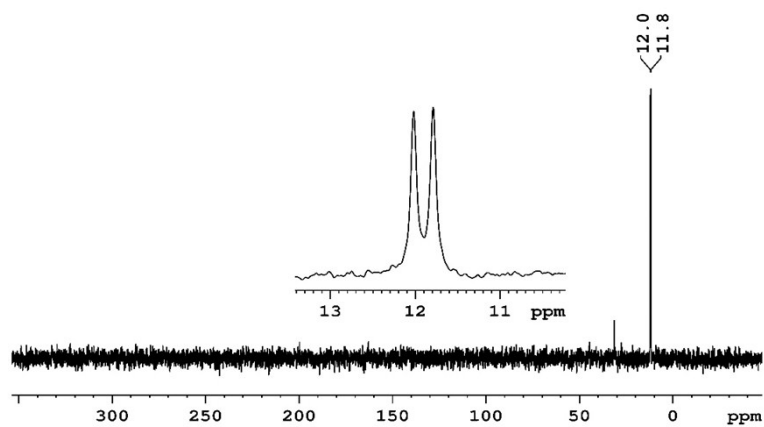


**Figure S14.**  $^{31}\text{P}\{{}^1\text{H}\}$ -NMR (202 MHz) spectrum of **2pF** in  $\text{C}_6\text{D}_6$ .

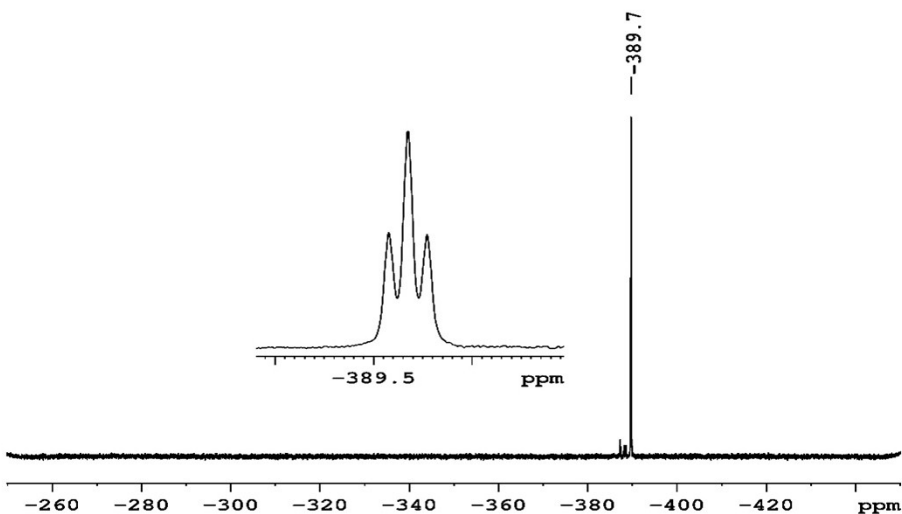


**Figure S15.**  $^{19}\text{F}$ -NMR (470 MHz) spectrum of **2pF** in  $\text{C}_6\text{D}_6$ .

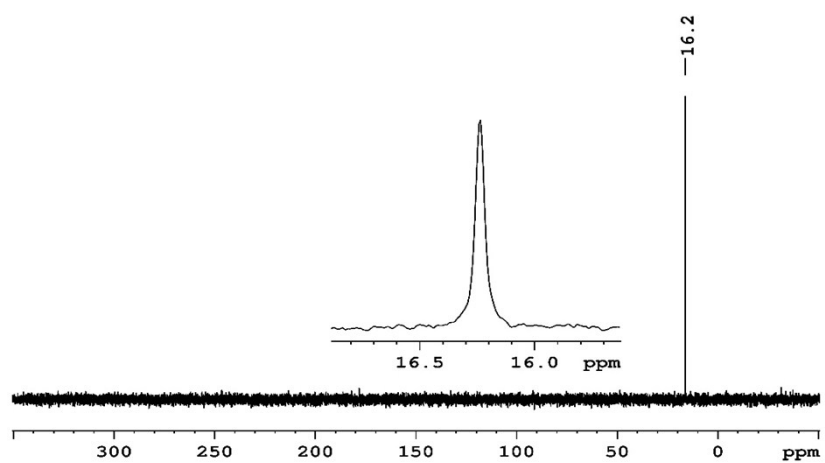


**Figure S16**  $^{31}\text{P}\{\text{H}\}$ -NMR (202 MHz) spectrum of **2pl** in  $\text{C}_6\text{D}_6$ .

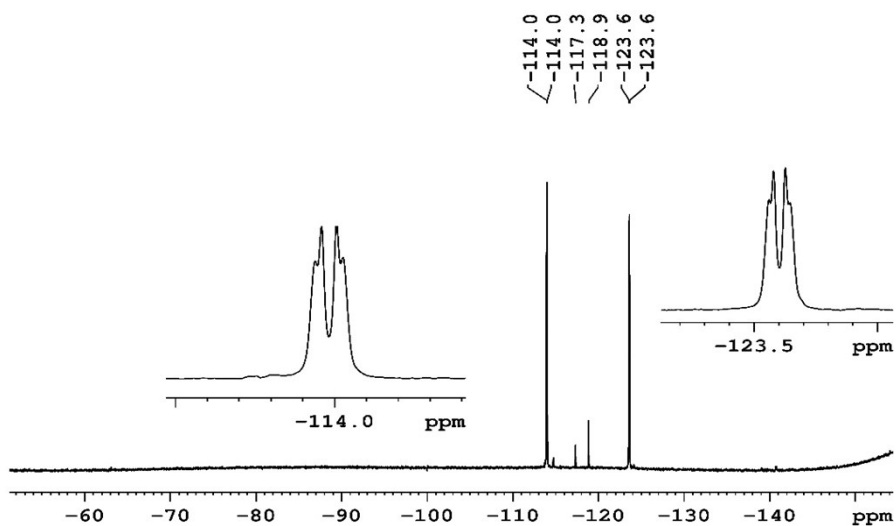


**Figure S17**  $^{19}\text{F}$ -NMR (470 MHz) spectrum of **2pl** in  $\text{C}_6\text{D}_6$ .

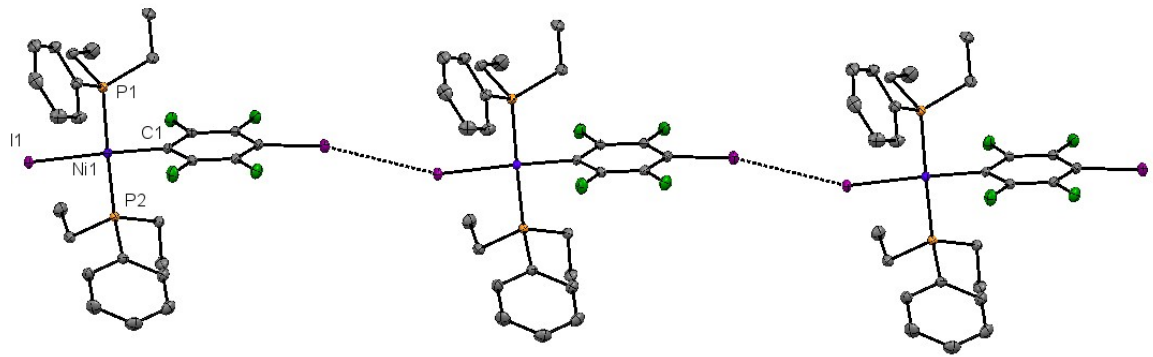


**Figure S18** Molecular structure of **2pl**. Displacement ellipsoids at 50% probability level.  
Hydrogen atoms are omitted for clarity.

**Table S8** Selected bond lengths ( $\text{\AA}$ ) and angles ( $^\circ$ ) of **2pl**.

I1-Ni1	2.5347(4)	C4-C5	1.381(4)
I2-C4	2.089(2)	C1-C6	1.387(3)
Ni1-P1	2.2194(6)	C5-C6	1.388(3)
Ni1-C1	1.901(2)	C4-C3	1.390(3)
P1-C7	1.839(2)	C4-I2…I1	167.4(7)
P2-C19	1.839(2)	I2…I1-Ni1	158.2(1)
F1-C2	1.354(2)	C9-P1-C16	105.8(1)
C7-C8	1.521(3)	I1-Ni1-C1	172.92(7)

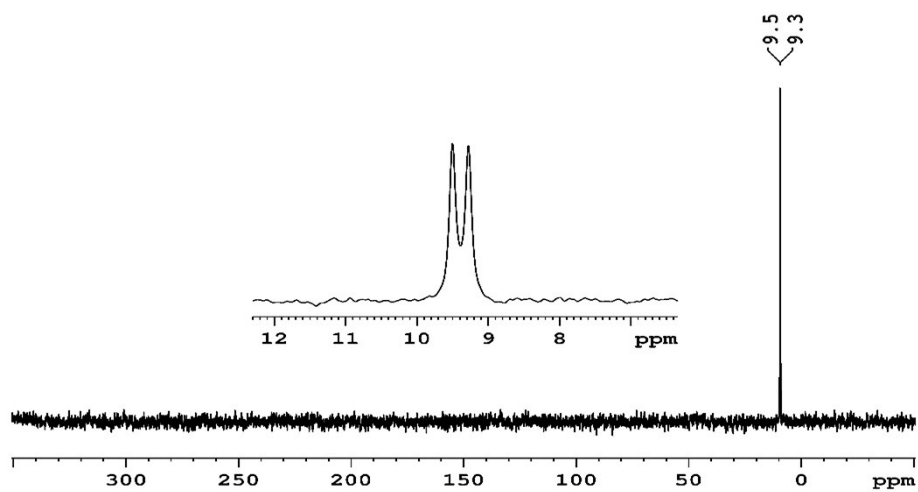


**Figure S19.**  $^{31}\text{P}\{^1\text{H}\}$ -NMR (202 MHz) spectrum of **1oF** in  $\text{C}_6\text{D}_6$ .

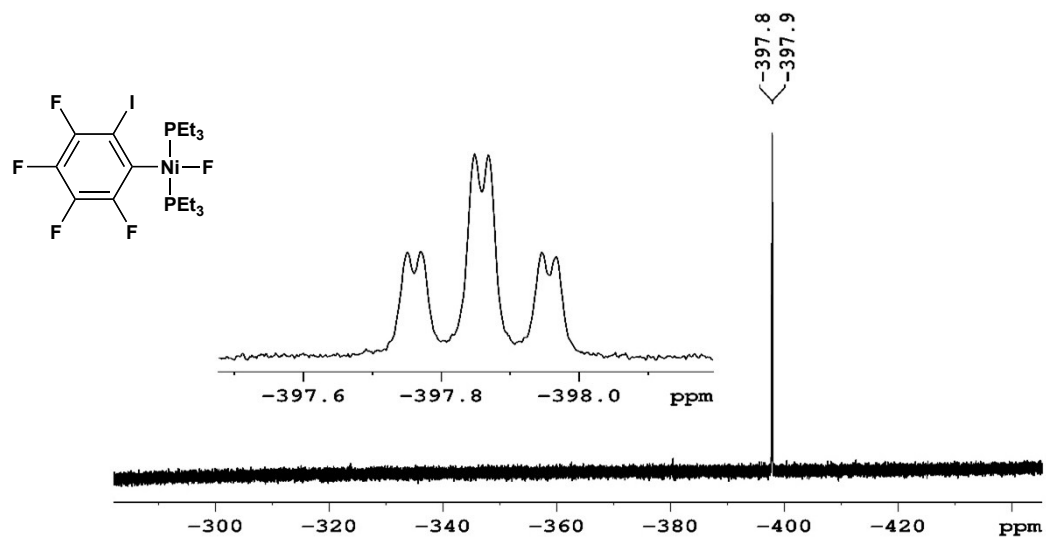


**Figure S20.**  $^{19}\text{F}$ -NMR (470 MHz) spectrum of **1oF** in  $\text{C}_6\text{D}_6$  in high field region.

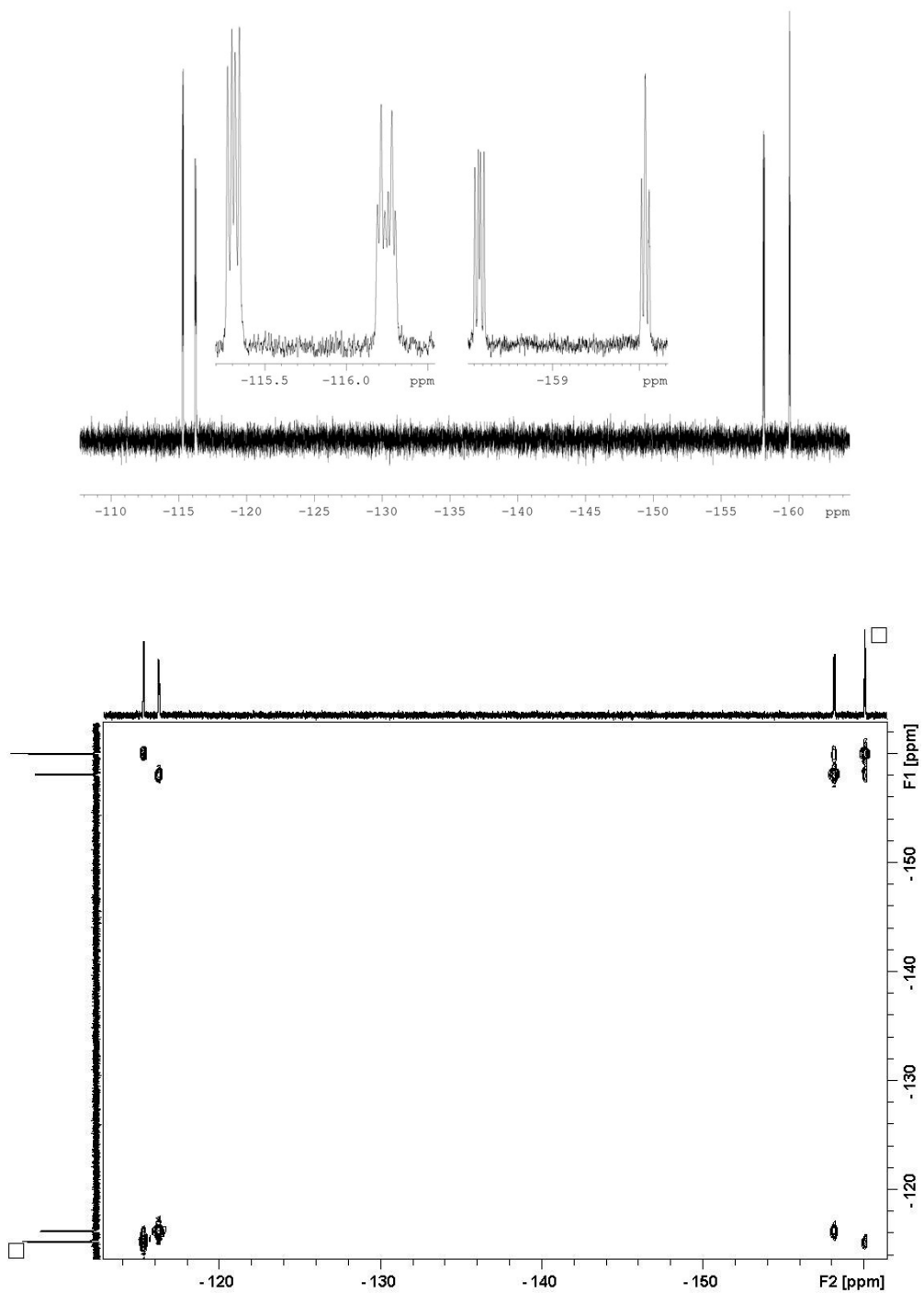


**Figure S21.**  ${}^{19}\text{F}$ -NMR (470 MHz) spectrum of **1oF** in  $\text{C}_6\text{D}_6$  in fluoroaromatic region: above  ${}^{19}\text{F}$  NMR spectrum, below  ${}^{19}\text{F}-{}^{19}\text{F}$  COSY spectrum.

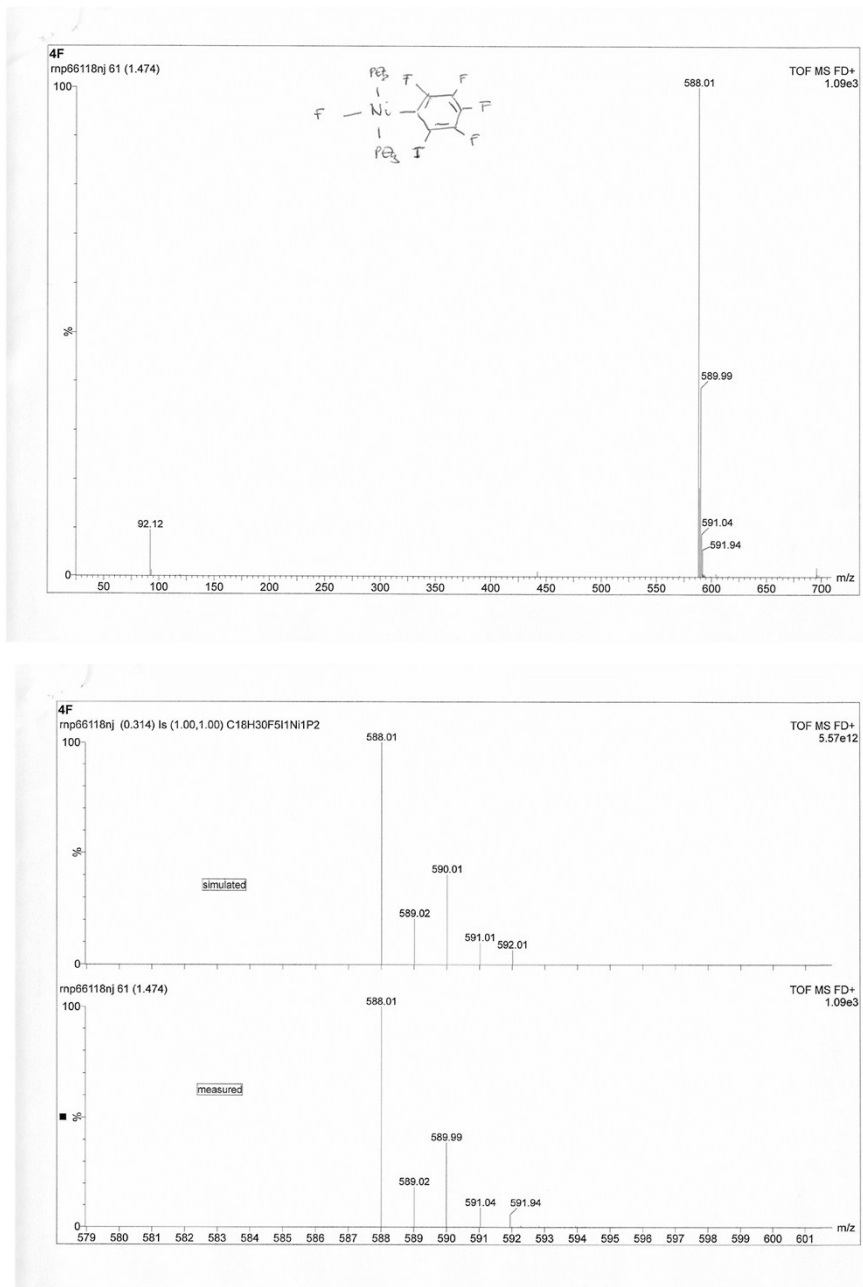


**Figure S22.** LIFDI mass spectrum of **1oF**. Above full spectrum. Below expansion and simulation.

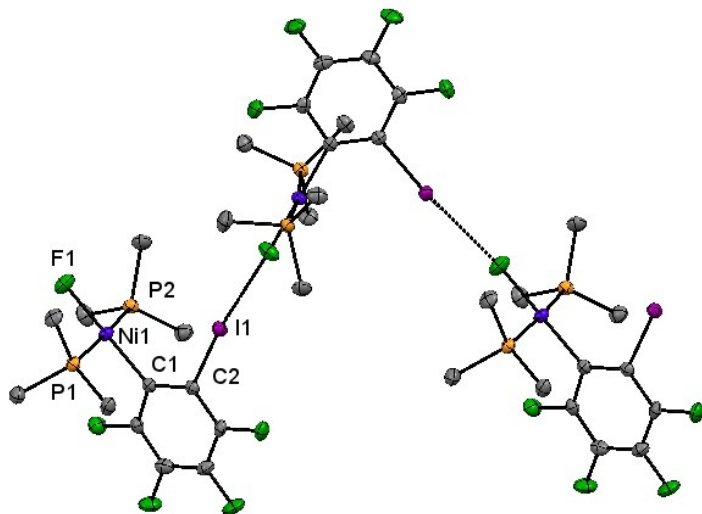


**Figure S23** Molecular structure of **1oF**. Displacement ellipsoids at 50% probability level. Hydrogen atoms and phosphine C( $\beta$ ) substituents are omitted for clarity.

**Table S9** Selected bond lengths ( $\text{\AA}$ ) and angles ( $^\circ$ ) of **1oF**.

C1-C2	1.39(1)	F1-Ni1	1.841(5)
C1-Ni1	1.891(7)	Ni1-P1	2.218(2)
C2-C3	1.39(1)	C1-C6	13.95(9)
C2-I1	2.110(7)	C7-P1	1.829(9)
C3-C4	1.39(1)	P1-Ni1-P2	173.12(8)
C3-F2	1.341(9)	F1-Ni1-C1	179.3(3)
C4-C5	1.35(1)	Ni1-F1...I1	172.4(3)
C4-F3	1.361(9)	C2-I1...F1	173.2(2)
C5-C6	1.38(1)	C7-P1-C11	104.5(4)

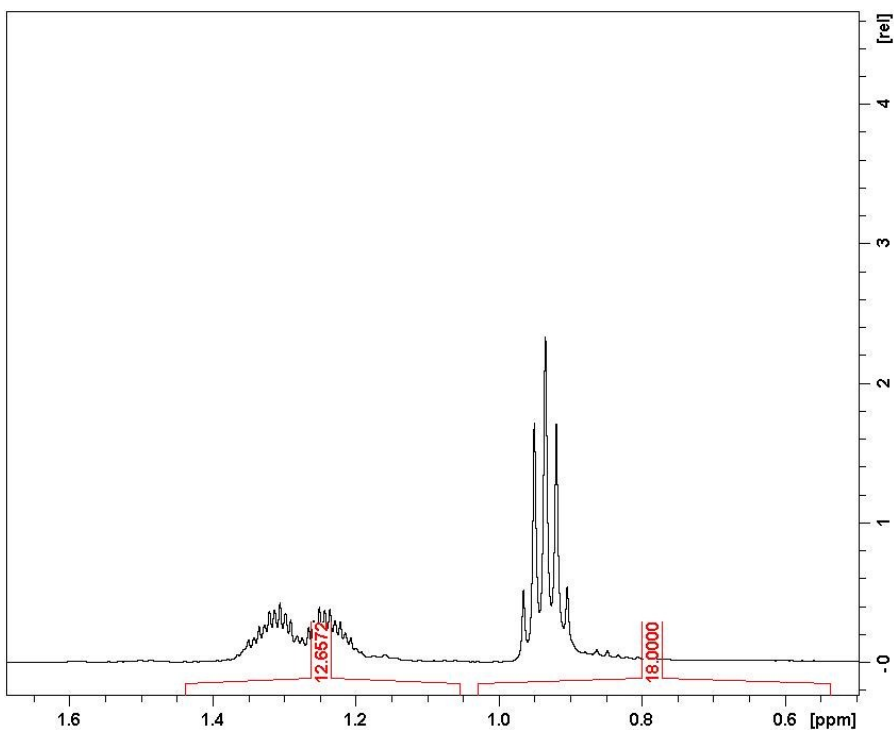


**Figure S24.**  ${}^1\text{H}$  NMR spectrum of **1oCl** in  $\text{C}_6\text{D}_6$ .

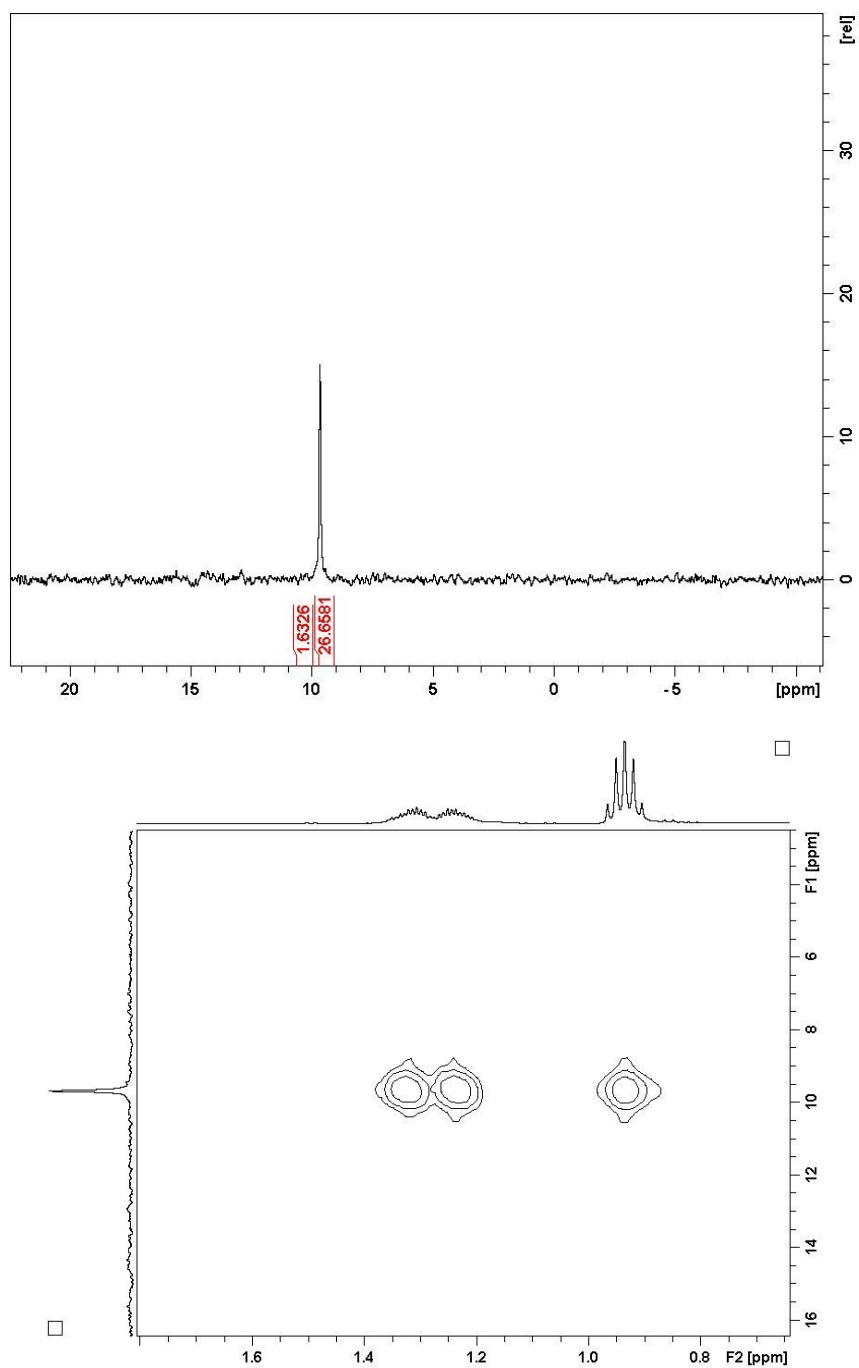


**Figure S25.**  ${}^{31}\text{P}\{{}^1\text{H}\}$  NMR spectrum (above) of **1oCl** in  $\text{C}_6\text{D}_6$  and  ${}^{31}\text{P}-{}^1\text{H}$  correlation (below).

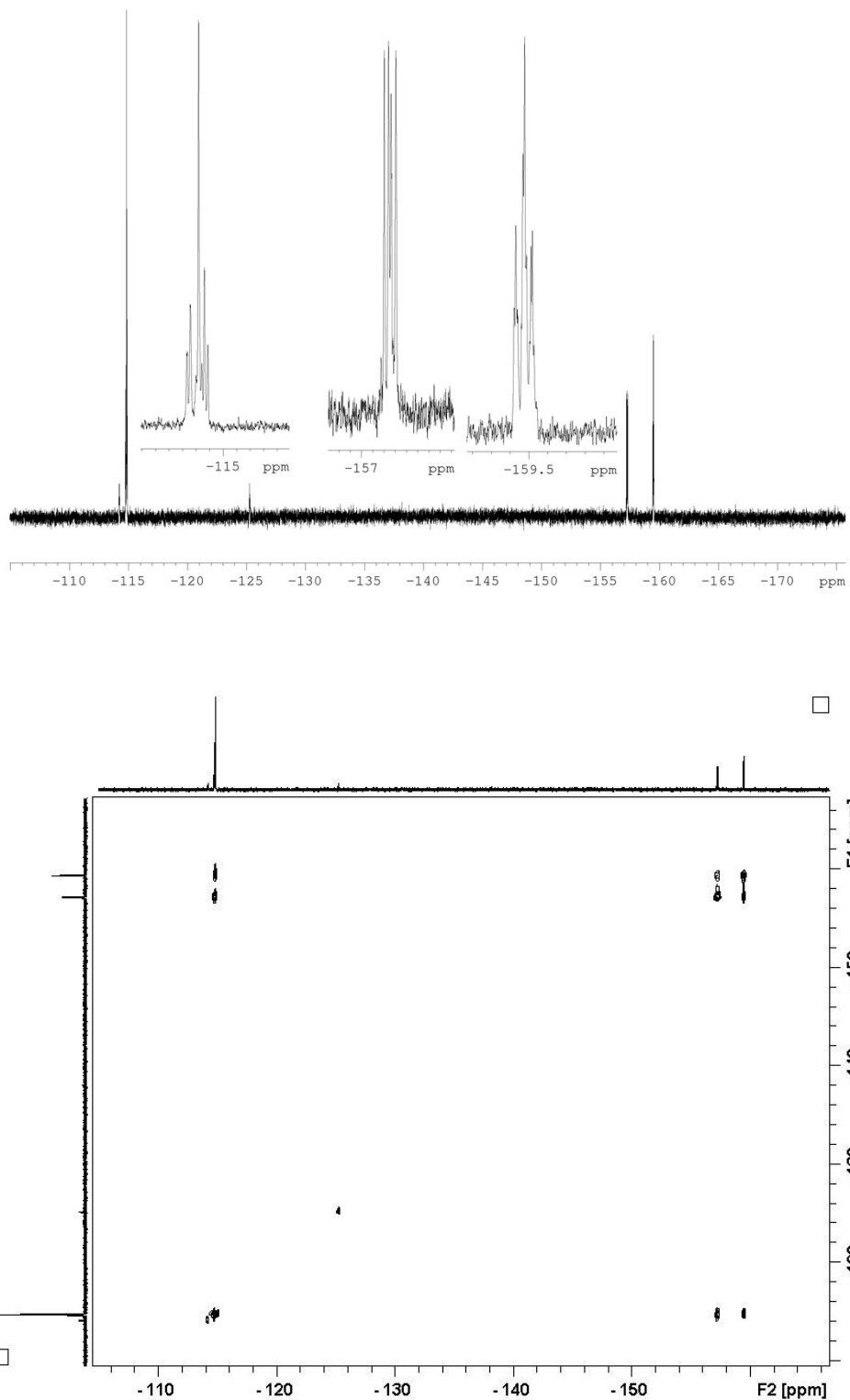


**Figure S26.**  ${}^{19}\text{F}$  NMR spectrum of **1oCl** in  $\text{C}_6\text{D}_6$ . Above  ${}^{19}\text{F}$  NMR, below  ${}^{19}\text{F}-{}^{19}\text{F}$  COSY

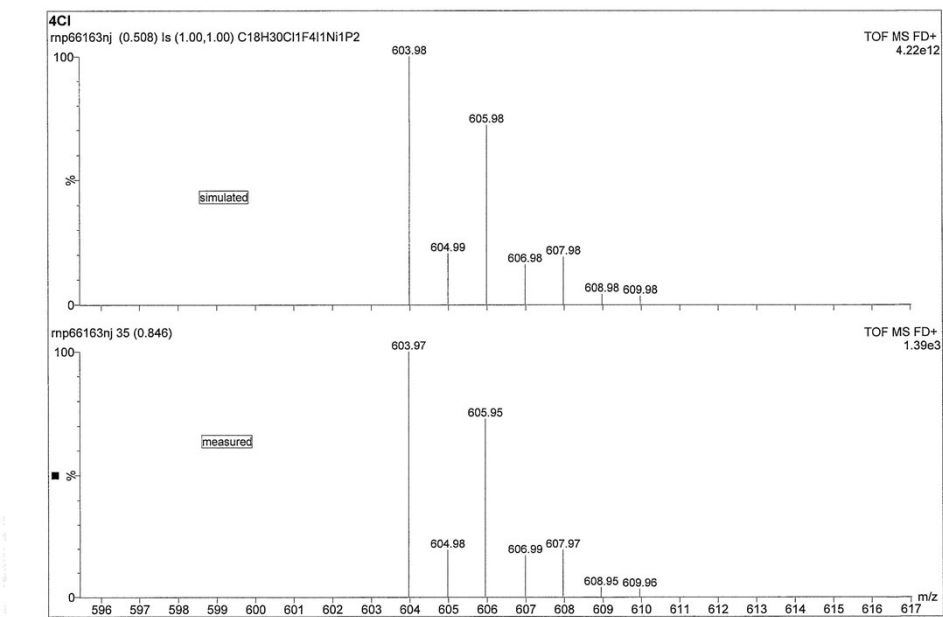
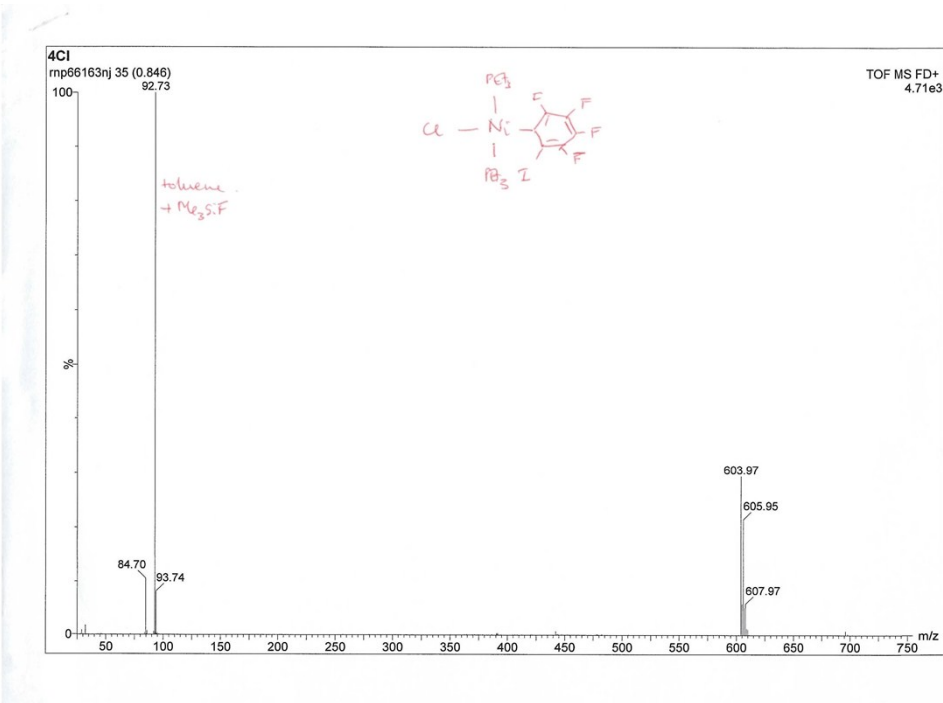


**Figure S27** LIFDI mass spectrum of **1oCl**. Above full spectrum. Below expansion and simulation.

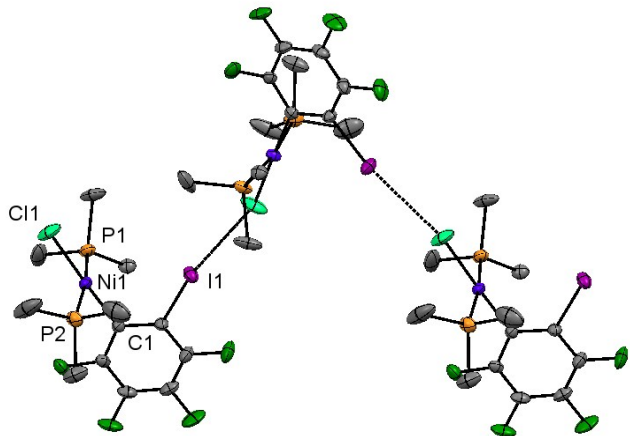


**Figure S28.** Molecular structure of **1oCl**. Thermal ellipsoids set at 50% level. Hydrogen atoms and the end methyl groups are omitted for clarity.

**Table S10.** Selected bond lengths ( $\text{\AA}$ ) and angles ( $^\circ$ ) of **1oCl**.

I1-C13	2.09(3)	I1-C13	2.09(3)
Ni2-P3	2.220(7)	Ni2-C12	1.88(2)
Ni2-C14	2.19(1)	F6-C5	1.34(4)
P3-C18	1.85(7)	C13-I1-Cl4	171.5(7)
F8-C9	1.32(3)	Ni2-Cl4-I1	160.7(5)

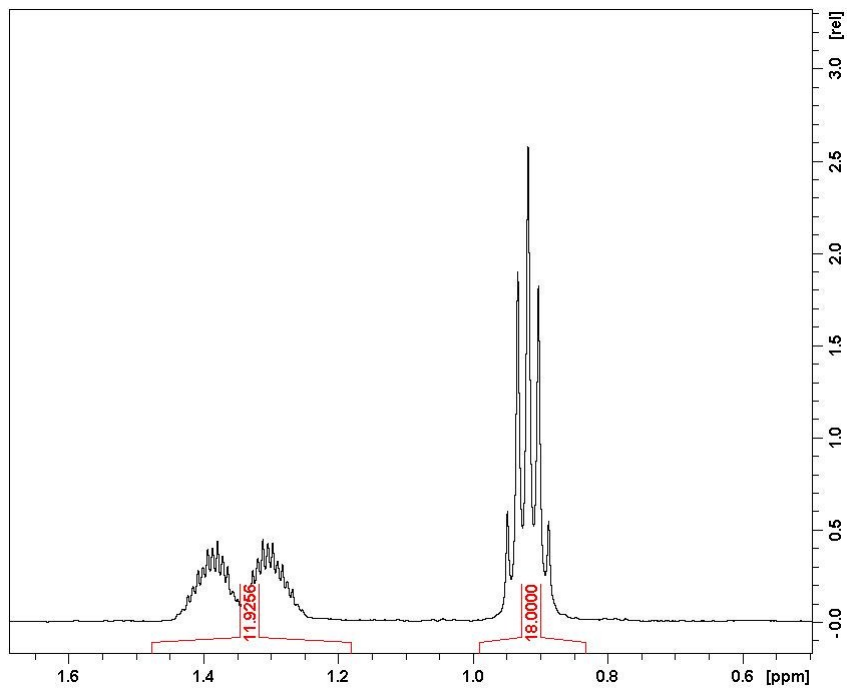


**Figure S29.**  ${}^1\text{H}$  NMR spectrum of **1oBr** in  $\text{C}_6\text{D}_6$ .

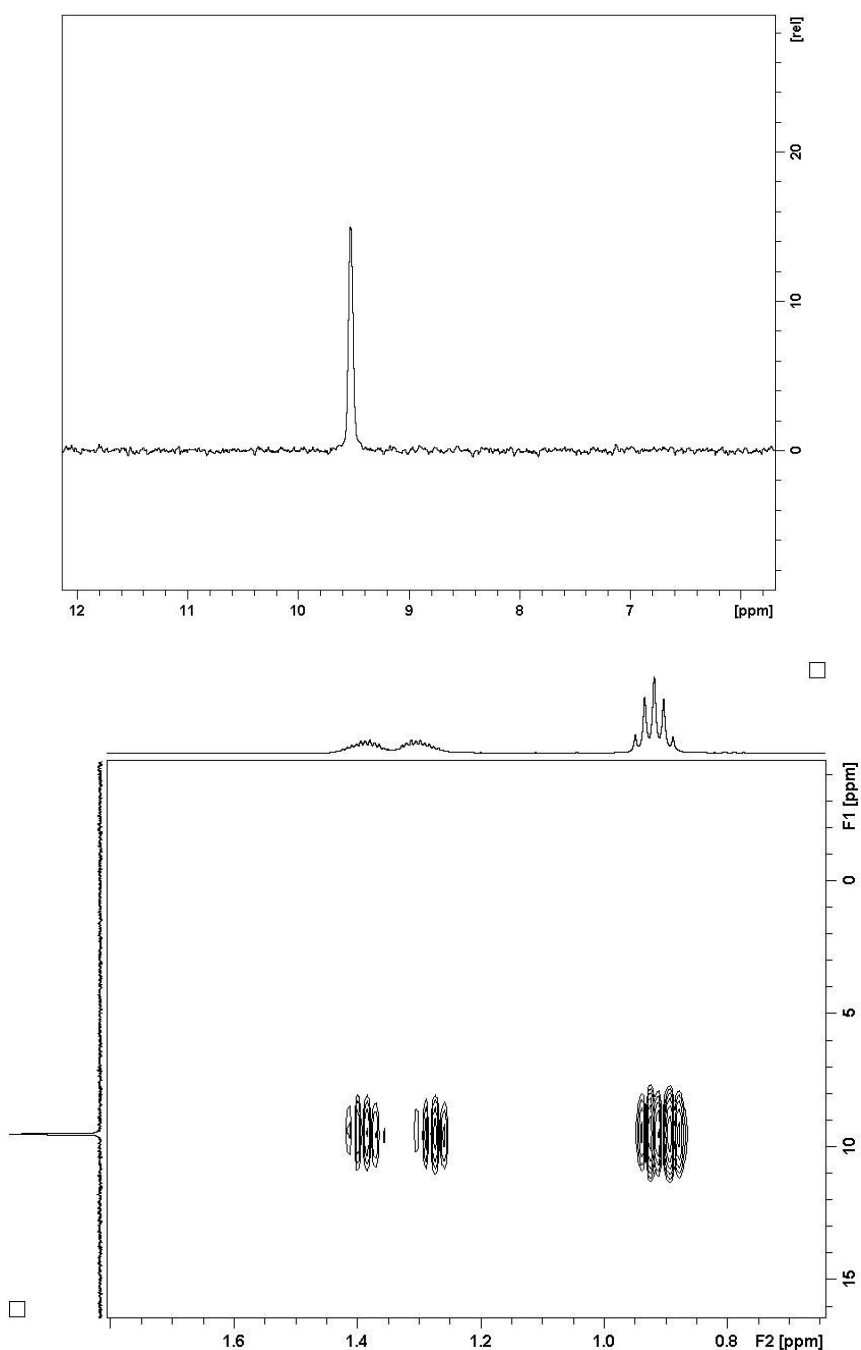


**Figure S30.**  ${}^{31}\text{P}\{\text{H}\}$  NMR spectrum (above) of **1oBr** in  $\text{C}_6\text{D}_6$  and  ${}^{31}\text{P}-\text{H}$  correlation (below)

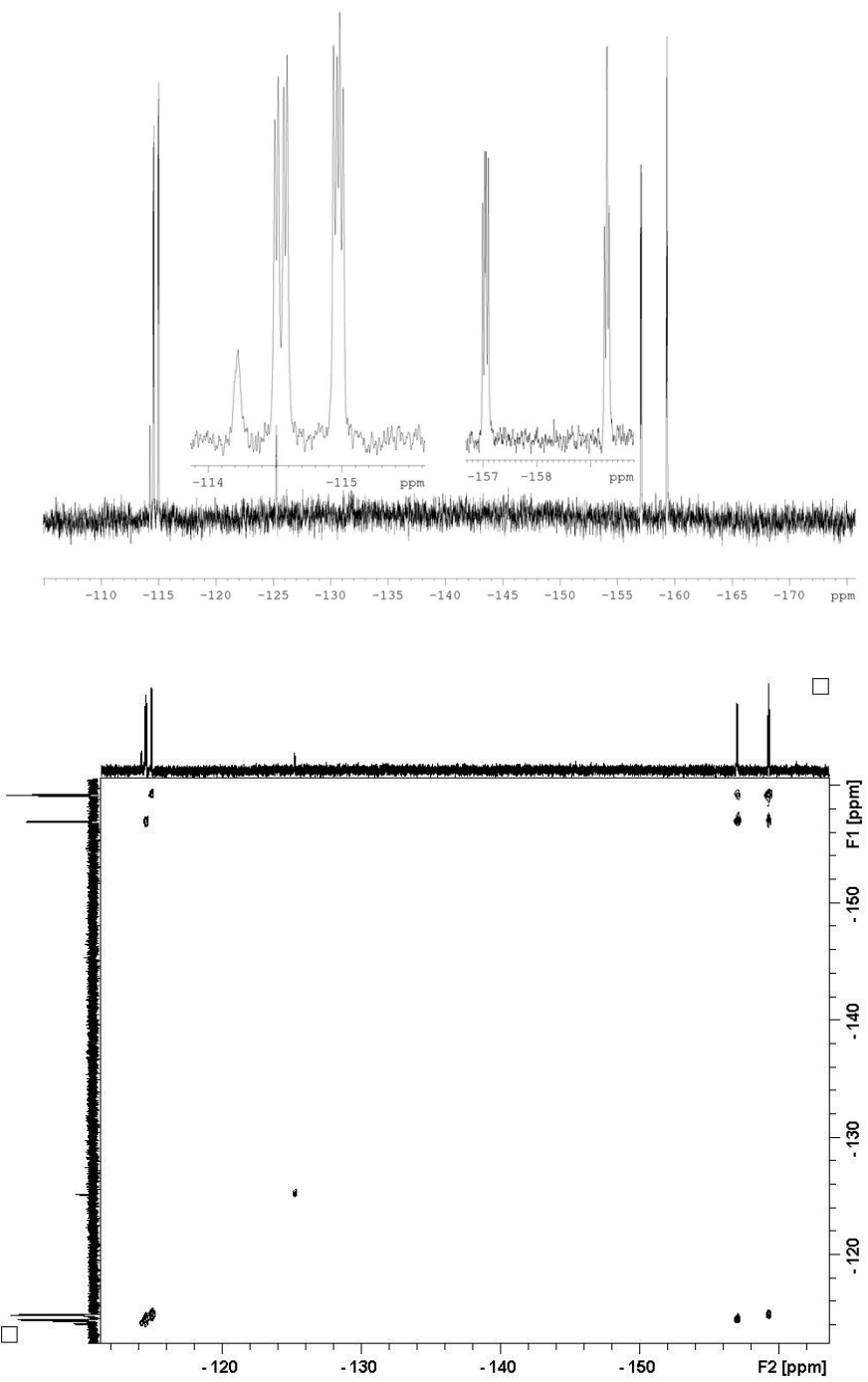


**Figure S31.**  ${}^{19}\text{F}$  NMR spectrum of **1oBr** in  $\text{C}_6\text{D}_6$ . Above  ${}^{19}\text{F}$  NMR, below  ${}^{19}\text{F}-{}^{19}\text{F}$  COSY

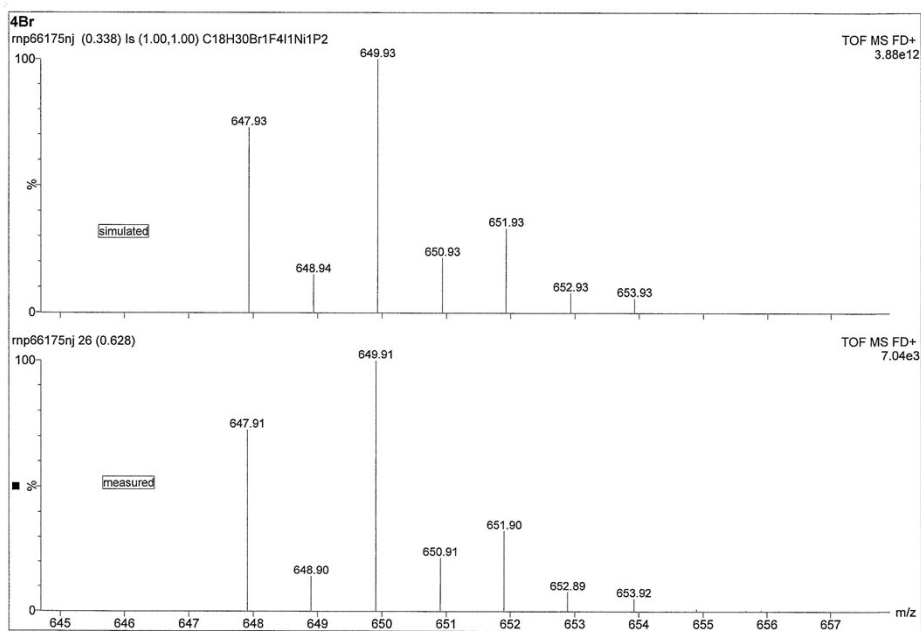
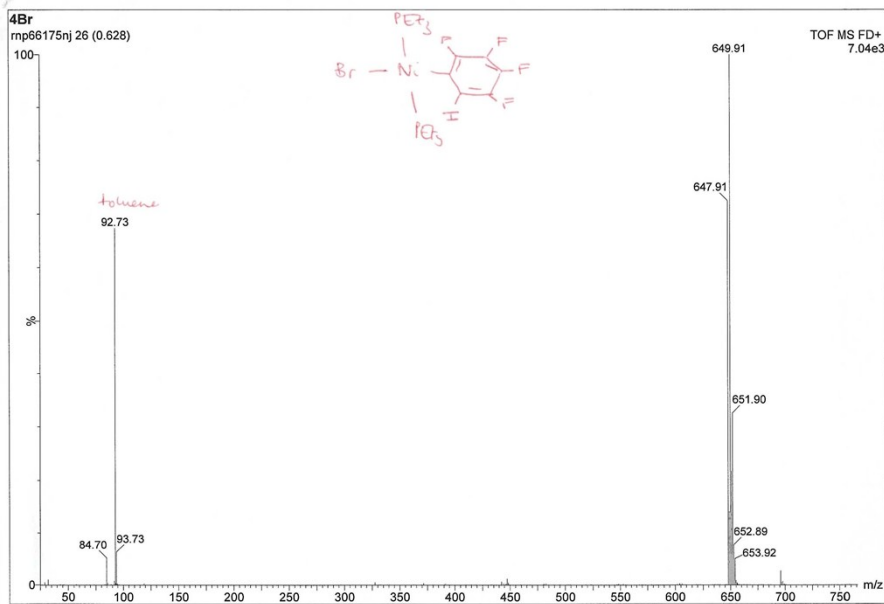


**Figure S32.** LIFDI mass spectrum of **1oBr**. Above full spectrum. Below expansion and simulation.

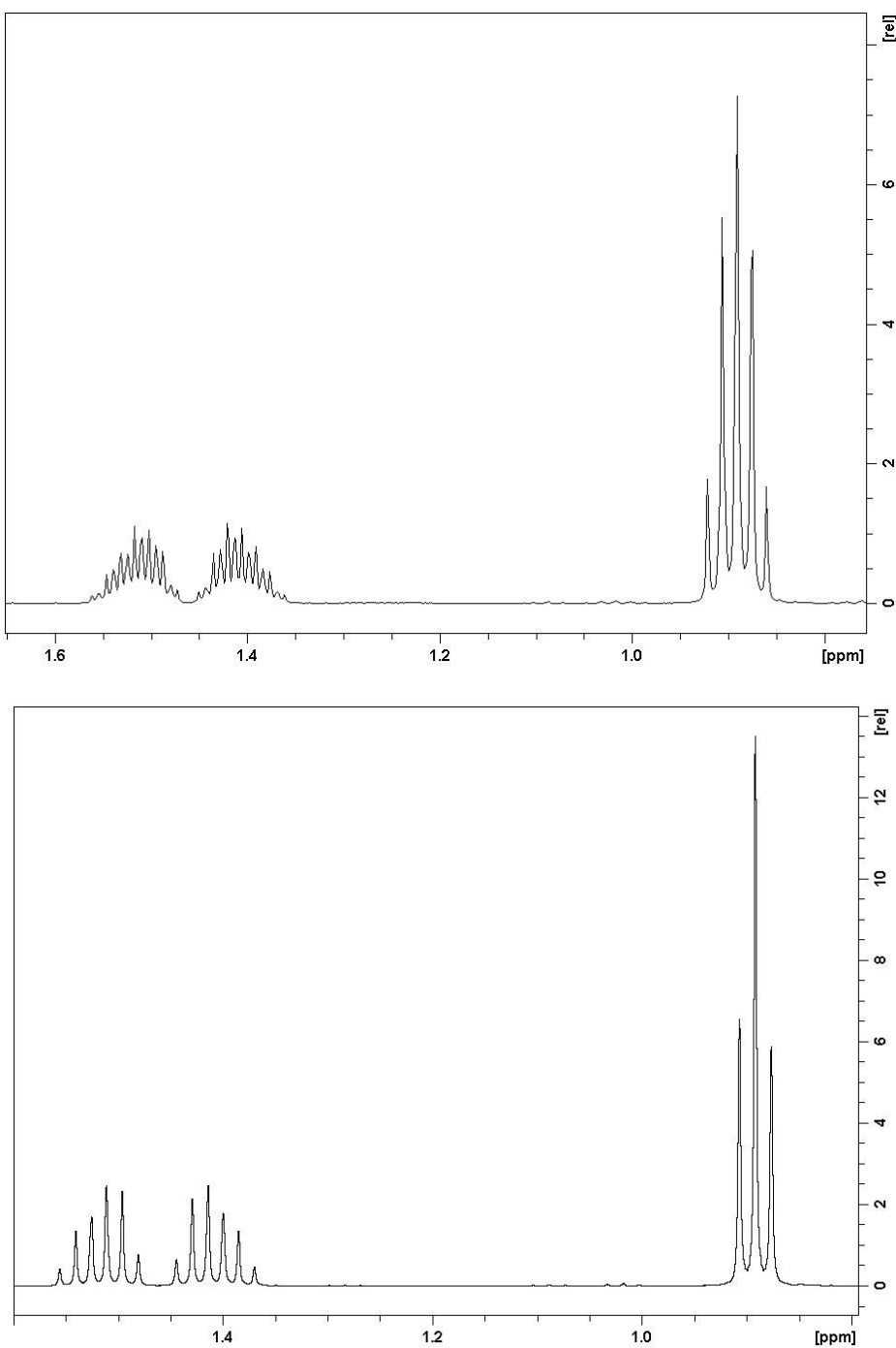


**Figure S33.** Above  $^1\text{H}$  NMR spectrum of **1ol** in  $\text{C}_6\text{D}_6$ . Below  $^1\text{H}\{^{31}\text{P}\}$  NMR of **1ol**.

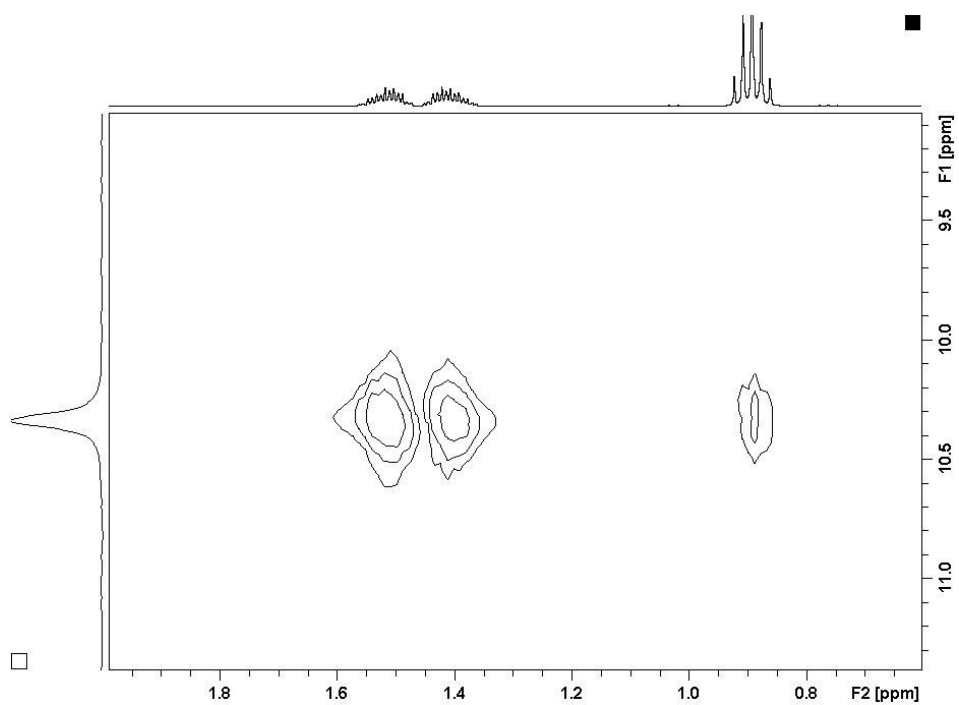


**Figure S34.**  $^1\text{H}$ - $^{31}\text{P}$  HMQC of **1ol**

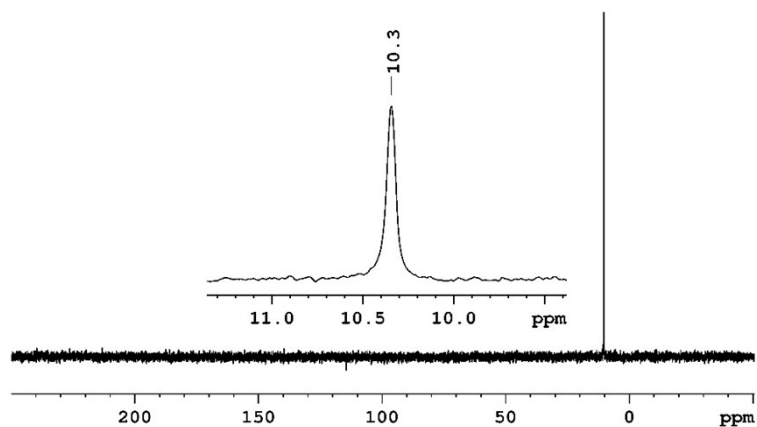


**Figure S35**  $^{31}\text{P}\{\mathbf{^1H}\}$ -NMR (202 MHz) spectrum of **1ol** in  $\text{C}_6\text{D}_6$ .

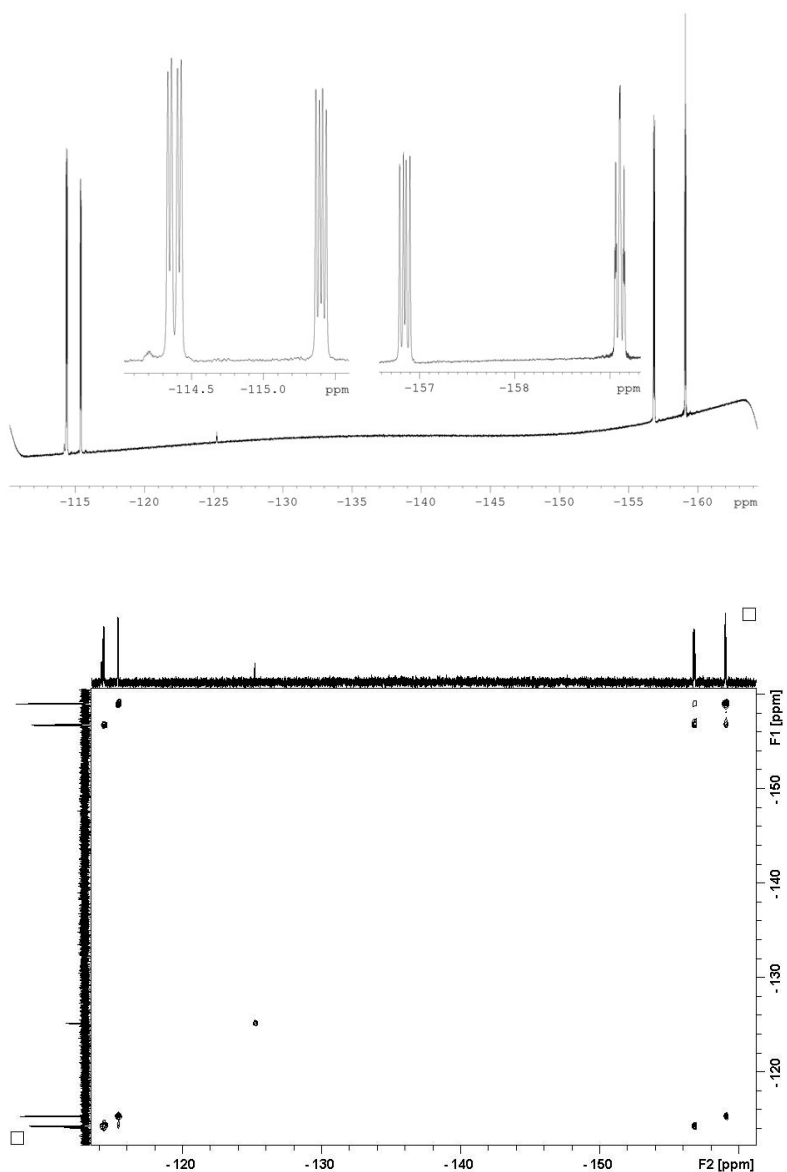


**Figure S36.** Above:  ${}^{19}\text{F}$ -NMR spectrum (470 MHz) spectrum of **10l** in  $\text{C}_6\text{D}_6$ . Below:  ${}^{19}\text{F}-{}^{19}\text{F}$  COSY spectrum

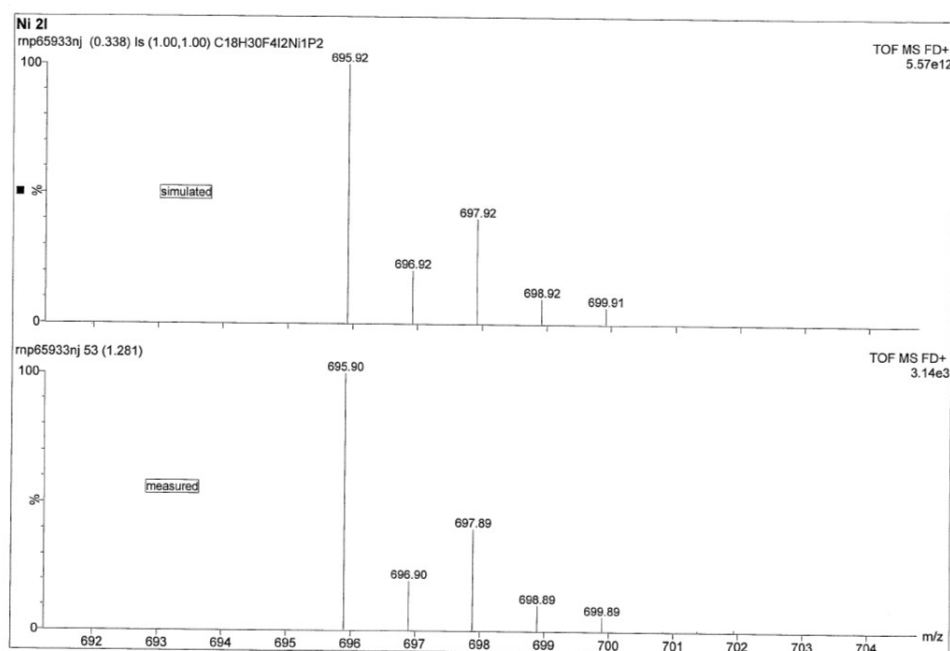
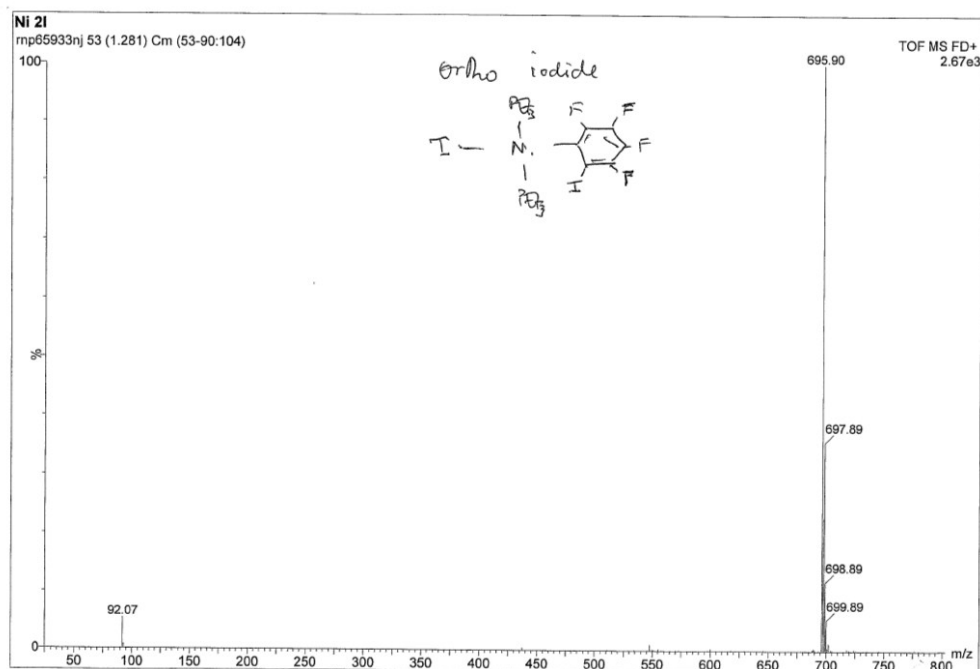


**Figure S37.** LIFDI mass spectrum of **1ol**. Above full spectrum. Below expansion and simulation.

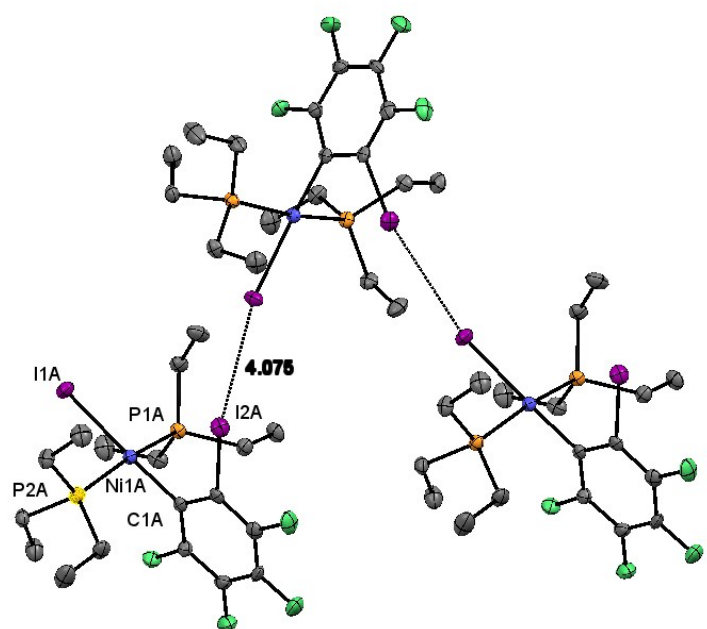
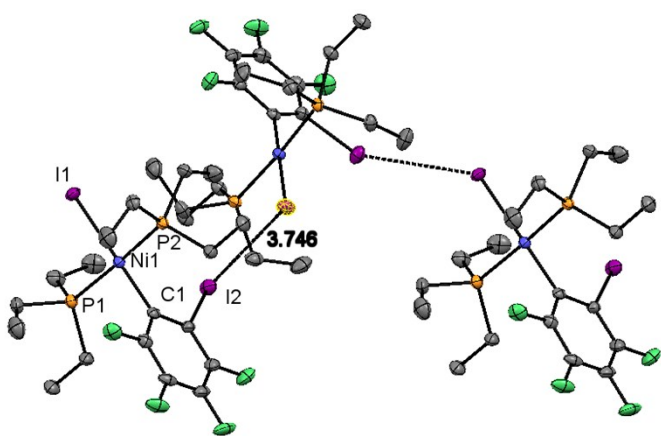
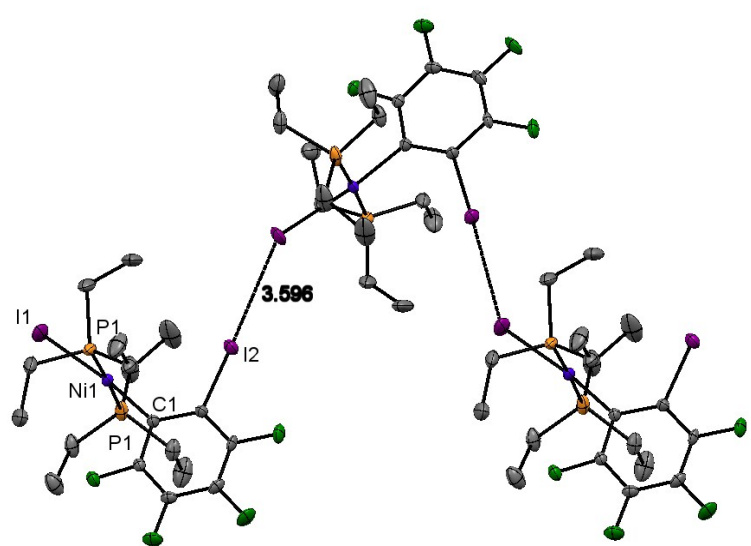


**Figure S38.** Molecular structure of **1ol**. Top: **1ol(α)** crystals grown from hexane. Middle: **1ol(β)** crystals grown from chloroform (only major component displayed). Bottom: **1ol(γ)** crystals grown from chloroform. The independent molecule in **1ol(γ)** which does not exhibit halogen bonding is not shown. Displacement ellipsoids at 50% probability level and hydrogen atoms are omitted for clarity. Halogen bond distances in Å.

**Table S11** Selected bond lengths (Å) and angles (°) of **1ol(α)**.

C1-C2	1.403(6)	Ni1-P1	2.2254(10)
C1-C6	1.385(6)	I1-Ni1	2.5332(6)
C1-Ni1	1.907(4)	C2-C3	1.381(6)
C2-I2	2.096(4)	C2-I2…I1	178.5(1)
C3-F1	1.359(5)	Ni-I1…I2	144.16(2)
C6-F4	1.357(6)	C7-P1-C9	103.8(2)
C7-P1	1.824(4)	I1-Ni1-C1	173.81(13)
C9-C10	1.521(7)	P1-Ni1-P1'	177.33(5)

**Table S12.** Crystal data for complexes **2pI**, **1oF**, **1oCl** and **1oI**

	<b>2pI</b>	<b>1oF</b>	<b>1oCl</b>	<b>1oI(α) grown from hexane</b>	<b>1oI(β) grown from CHCl<sub>3</sub></b>	<b>1oI(γ) grown from CHCl<sub>3</sub></b>
CCDC	1825446	1825447	1825448	1825449	1825451	1825450
Formula	C <sub>26</sub> H <sub>30</sub> F <sub>4</sub> I <sub>2</sub> NiP <sub>2</sub>	C <sub>18</sub> H <sub>30</sub> F <sub>5</sub> INiP <sub>2</sub>	C <sub>18</sub> H <sub>30</sub> ClF <sub>4</sub> INiP <sub>2</sub>	C <sub>18</sub> H <sub>30</sub> F <sub>4</sub> I <sub>2</sub> NiP <sub>2</sub>	C <sub>18</sub> H <sub>30</sub> F <sub>4</sub> I <sub>2</sub> NiP <sub>2</sub>	C <sub>18</sub> H <sub>30</sub> F <sub>4</sub> I <sub>2</sub> NiP <sub>2</sub>
M	792.95	588.97	605.42	696.87	696.87	696.87
a/ Å	7.8141(3)	9.4116(5)	9.2736(2)	12.6196(2)	14.0554(2)	12.19004(19)
b/ Å	12.9211(4)	12.7010(8)	13.2118(3)	14.8011(4)	14.4542(2)	28.0191(5)
c/ Å	14.7784(5)	9.7270(5)	9.8170(2)	13.2994(2)	24.3397(5)	14.2344(2)
V/ Å <sup>3</sup>	1401.12(9)	1157.62(11)	1197.81(5)	2484.11(9)	4944.85(15)	4859.88(13)
T/ K	110	110	110	110	110	110
α /°	76.749(3)	90	90	90	90	90
β /°	79.700(3)	95.365(8)	95.220(2)	90	90	91.6129(13)
γ /°	76.748(3)	90	90	90	90	90

Space gp	P-1	P2 <sub>1</sub>	P2 <sub>1</sub>	Cmc2 <sub>1</sub>	Pbca	P2 <sub>1</sub> /c
Z	2	2	2	4	8	8
Reflections collected	17424	7725	10869	8209	23320	18154
Independent reflections	8876	7725	6245	3532	7817	8677
Final R [ $I \geq 2\sigma(I)$ ]	$R_1 = 0.0248$ $wR_2 = 0.0526$	$R_1 = 0.0333$ $wR_2 = 0.0846$	$R_1 = 0.0288$ $wR_2 = 0.0636$	$R_1 = 0.0204$ $wR_2 = 0.0434$	$R_1 = 0.0290$ $wR_2 = 0.0534$	$R_1 = 0.0358$ $wR_2 = 0.0858$
Final R [all data]	$R_1 = 0.0310$ $wR_2 = 0.0566$	$R_1 = 0.0333$ $wR_2 = 0.0845$	$R_1 = 0.0288$ $wR_2 = 0.0636$	$R_1 = 0.0220$ $wR_2 = 0.0447$	$R_1 = 0.0429$ $wR_2 = 0.0593$	$R_1 = 0.0429$ $wR_2 = 0.0904$
Flack parameter	n/a	0.466(14)	0.156(18)	-0.004(11)	n/a	n/a

**Refinement of crystal structures of **1oX**.** The crystal of **1oF** was non-merohedrally twinned and modelled as a two-component system using CrysAlisPro. The ratio of the components refined to 0.542:0.458 (1). There was also evidence of racemic twinning but it was not possible to model both non-merohedral and merohedral twinning at the same time.

The crystal of **1oCl** exhibited two forms of disorder. Firstly, the nickel and chlorine were disordered and modelled in two positions with occupancies of 0.73:0.27(2). The nickel atoms were constrained to have identical ADPs as were the chlorine atoms. Secondly, one of the triethylphosphine ligands was disordered, with each ethyl group being modelled in two positions (occupancies 0.605:0.395(6)). For one of the ethyl groups the methyl carbons occupied the same site. Each pair of methyl carbons was constrained to have a common set of ADPs. The C–C distances in the disordered ethyls were restrained to 1.52 Å. The crystal was also racemically twinned with the ratio of the two components refined to 0.84:0.16(2).

The crystal of **1oI(β)** exhibited disorder with the iodine (I1) and aromatic ring modelled in two positions differing by 180° rotation about an axis close to the I1–Ni–C1 axis and refined occupancies of 0.931:0.069(1). The aromatic ring of the minor form was constrained to be a regular hexagon with C–C bond lengths of 1.39 Å. The ADPs of atoms of the minor form were constrained to be the same as those of the adjacent atoms of the major form (ie. C2 & C6a I2 & F4a, I1 & I1a, etc).

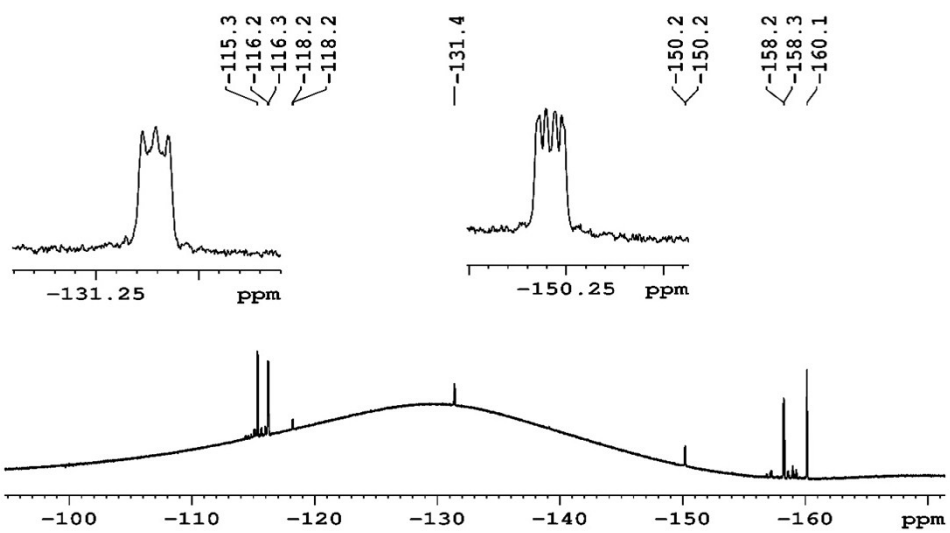


**Figure S39.**  $^{19}\text{F}$ -NMR (470 MHz) spectrum of the sample containing  $\text{Ni}(\text{PEt}_3)_2(\text{C}_6\text{F}_4)$ .

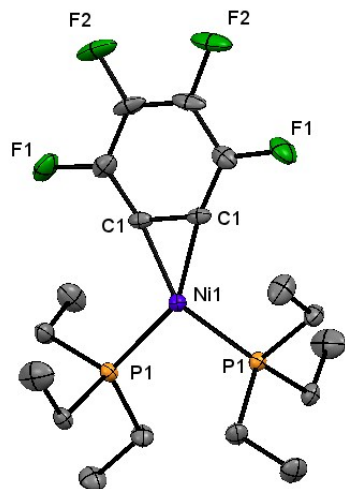


**Figure S40.** Molecular structure of  $\text{Ni}(\text{PEt}_3)_2(\eta^2\text{-C}_6\text{F}_4)$ . Thermal ellipsoids set at 50% level and hydrogen atoms are omitted for clarity.

**Table S13.** Selected Bond lengths (Å) and angles (°) of Ni(PEt<sub>3</sub>)<sub>2</sub>(C<sub>6</sub>F<sub>4</sub>)

C1-C2	1.364(5)	C2-C1-C1'	121.6(3)
C1-C1	1.359(5)	Ni1-C1-C1'	68.70(10)
C2-C3	1.386(5)	C1-Ni1-P1	106.28(10)
C3-C3'	1.385(8)	C1-Ni1-C1'	42.61
C2-F1	1.365(4)	C1-Ni1-P1	148.88
C3-F2	1.356(4)	C1-C1'-Ni-P1'	-1.5(4)
C4-P1	1.824(3)	P1-P1'-C1-C1'	1.05
Ni1-P1	2.1684(9)		
Ni1-C1	1.870(3)		

**Table S14** Crystal data for  $\text{Ni}(\text{PEt}_3)_2(\text{C}_6\text{F}_4)$  and  $[\text{trans-NiBr}(\text{PEt}_3)_2]_2(\mu\text{-2,3,5,6-C}_6\text{F}_4)$ 

	$\text{Ni}(\text{PEt}_3)_2(\text{C}_6\text{F}_4)$	$[\text{trans-NiBr}(\text{PEt}_3)_2]_2(2,3,5,6\text{-C}_6\text{F}_4)$
CCDC	1825452	1825404
formula	$\text{C}_{18}\text{H}_{30}\text{F}_4\text{NiP}_2$	$\text{C}_{30}\text{H}_{60}\text{Br}_2\text{F}_4\text{Ni}_2\text{P}_4$
M	443.07	897.92
a/ Å	8.13398(18)	11.0590(5)
b/ Å	8.13398(18)	12.1681(6)
c/ Å	31.6136(10)	15.1847(8)
V/ Å <sup>3</sup>	2091.61(11)	1982.25(10)
T/ K	110	123
$\alpha /^\circ$	90	75.960(3)
$\beta /^\circ$	90	89.526(2)
$\gamma /^\circ$	90	89.997(2)
Space gp	P4 <sub>3</sub> 2 <sub>1</sub> 2	P-1
Z	4	2
Reflections collected	6224	8104
Independent reflections	3289	8071
Final R [I ≥ 2σ(I)]	R <sub>1</sub> = 0.0549	R <sub>1</sub> = 0.0252
	wR <sub>2</sub> = 0.0860	wR <sub>2</sub> = 0.0609
Final R [all data]	R <sub>1</sub> = 0.0637	R <sub>1</sub> = 0.0283
	wR <sub>2</sub> = 0.0890	wR <sub>2</sub> = 0.0627
Flack parameter	0.043(10)	n/a

### **Crystallographic Method for [trans-NiBr(PEt<sub>3</sub>)<sub>2</sub>]<sub>2</sub>(μ-2,3,5,6-C<sub>6</sub>F<sub>4</sub>)**

The X-ray intensities of the dimer were measured on a Bruker APEX II diffractometer using Incoatec microsource (Mo-K $\alpha$  radiation;  $\lambda = 0.71073 \text{ \AA}$ ) and an Oxford Cryosystems low temperature device operating at 123 K as standard.<sup>1</sup> Absorption corrections were carried out using the multiscan procedure SADABS.<sup>2</sup> The structures were solved by charge-flipping methodology (SUPERFLIP) and refined by full-matrix least-squares against  $F^2$  using all data (CRYSTALS).<sup>3</sup> H atoms were located in difference maps and initially refined with soft restraints on the bond lengths and angles to regularise their geometry (C-H in the range 0.93–0.98, N-H in the range 0.86–0.89  $\text{\AA}$ ) and  $U_{\text{iso}}$  (H) (in the range 1.2–1.5 times  $U_{\text{eq}}$  of the parent atom), after which the positions were refined with riding constraints. All non-H atoms were modelled with anisotropic displacement parameters

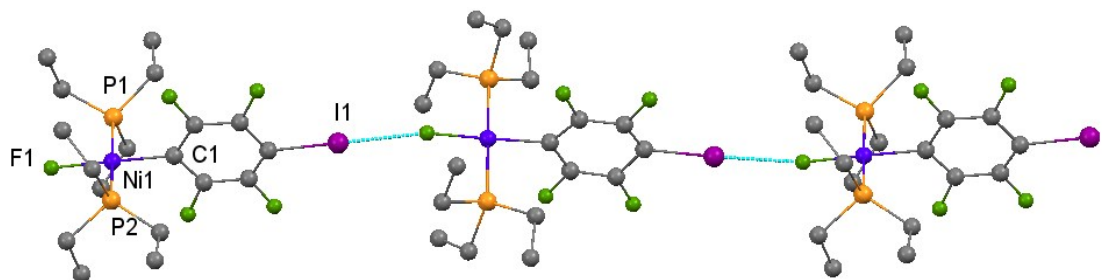
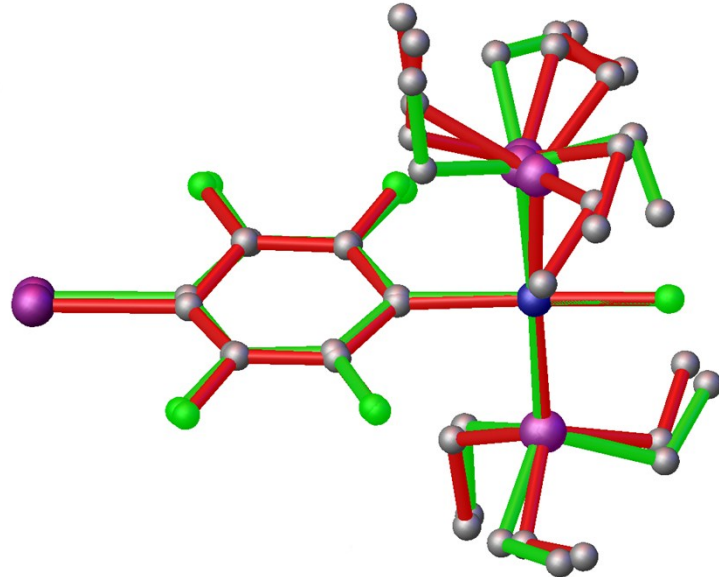


**Figure S41.** Top: Overlay of structures of **1pF** at 200 K (red) and 240 K (green). Bottom: Halogen-bonded chain in structure of **1pF** at 240 K. Hydrogen atoms and minor component of the disordered phosphine ligand omitted for clarity.

**Table S15** Crystal data and structure refinement for **1pF** at various temperatures.

T / K	110	200	240
CCDC	1825440	1825441	1825442
Crystal system	monoclinic	monoclinic	monoclinic
Space group	I2	I2	Cc
a/Å	7.8920(5)	8.0074(4)	17.1652(15)
b/Å	11.3325(4)	11.3665(4)	8.5185(13)
c/Å	12.9439(5)	12.9665(5)	16.935(2)
$\alpha/^\circ$	90	90	90
$\beta/^\circ$	94.434(5)	94.616(4)	96.803(10)
$\gamma/^\circ$	90	90	90
V/Å <sup>3</sup>	1154.19(9)	1176.34(8)	2458.8(5)
Z	2	2	4
Reflections collected	4467	4258	5903
Goodness-of-fit on F <sup>2</sup>	0.969	1.035	1.077
Final R [I ≥ 2σ(I)]	R <sub>1</sub> = 0.0312, wR <sub>2</sub> = 0.0611	R <sub>1</sub> = 0.0287, wR <sub>2</sub> = 0.0783	R <sub>1</sub> = 0.0559, wR <sub>2</sub> = 0.1623
Final R indexes [all data]	R <sub>1</sub> = 0.0364, wR <sub>2</sub> = 0.0622	R <sub>1</sub> = 0.0312, wR <sub>2</sub> = 0.0801	R <sub>1</sub> = 0.0769, wR <sub>2</sub> = 0.1825

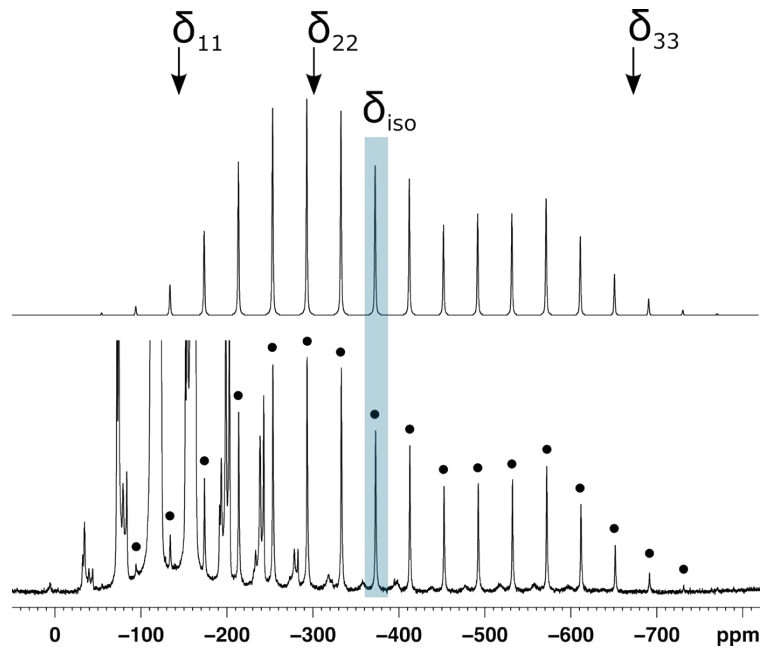


**Figure S42.** <sup>19</sup>F-MAS SSNMR spectrum of complex **1oF**. Top: best fit simulated spectrum for the Ni–F resonance with the positions of the shielding tensor marked. Bottom: experimental spectrum. Signals arising from the fluorinated benzene ligand (−80 to −200 ppm) are truncated. The black dots indicate the peaks corresponding to the fluoride resonance.

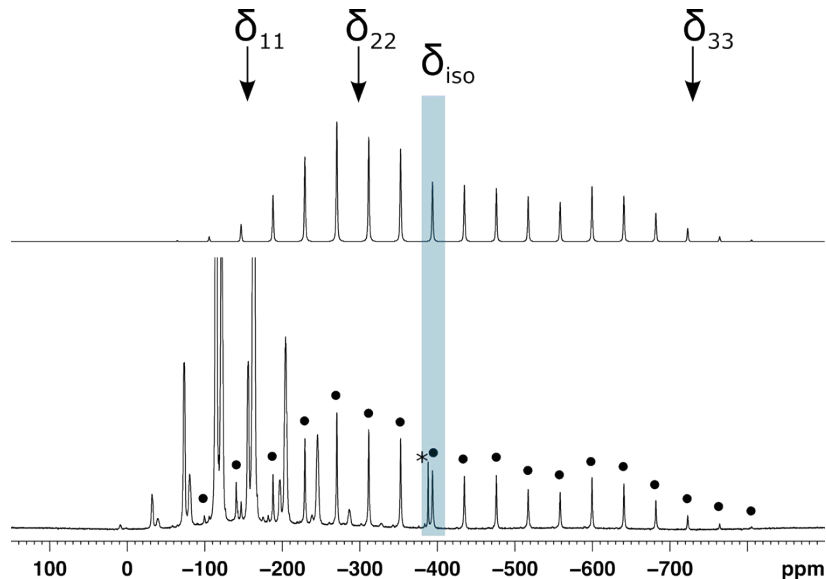


**Figure S43** <sup>19</sup>F-MAS SSNMR spectrum of **3F** *trans*-NiF(C<sub>6</sub>F<sub>5</sub>)(PEt<sub>3</sub>)<sub>2</sub>. Top: best fit simulated spectrum for the Ni–F resonance with the positions of the shielding tensor marked. Bottom: experimental spectrum. Signals arising from the fluorinated benzene ligand (−110 to −160 ppm) are truncated. The black dots indicate the peaks corresponding to the fluoride resonance.

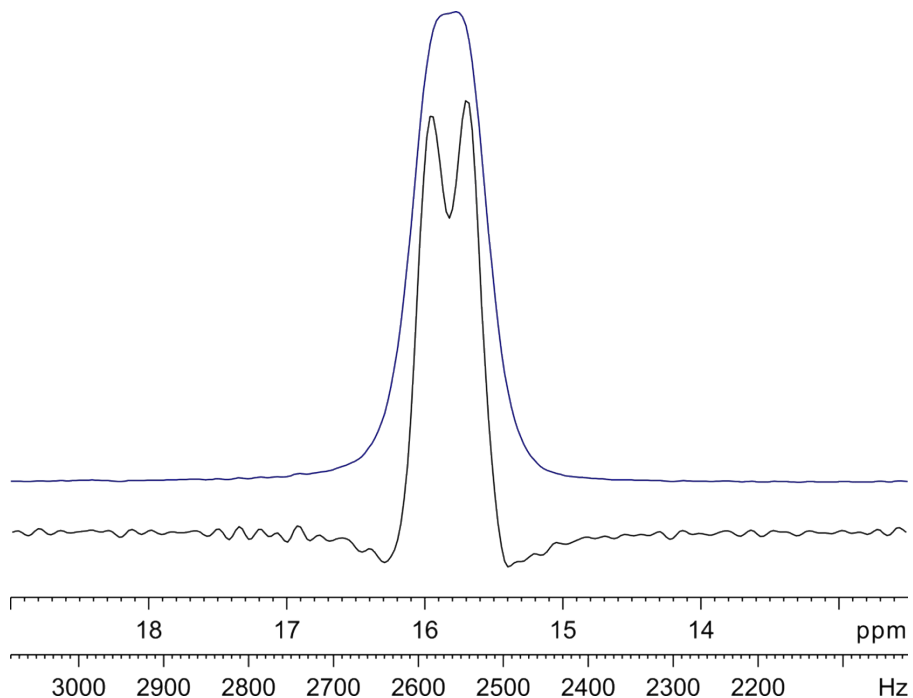


**Figure S44.**  $^{31}\text{P}\{^1\text{H}\}$  CPMAS spectrum of **1pF**. The lineshape hints at the presence of two peaks, which are resolvable using Lorentz-Gaussian apodization (LB = -50 Hz, GB = 0.8) allowing measurement of  ${}^2J(^{31}\text{P}, {}^{19}\text{F}) = 42 \pm 3$  Hz.

#### Gaussian Reference:

Gaussian 09, Revision B.01, M. J. Frisch, G. W. Trucks, H. B. Schlegel, G. E. Scuseria, M. A. Robb, J. R. Cheeseman, G. Scalmani, V. Barone, B. Mennucci, G. A. Petersson, H. Nakatsuji, M. Caricato, X. Li, H. P. Hratchian, A. F. Izmaylov, J. Bloino, G. Zheng, J. L. Sonnenberg, M. Hada, M. Ehara, K. Toyota, R. Fukuda, J. Hasegawa, M. Ishida, T. Nakajima, Y. Honda, O. Kitao, H. Nakai, T. Vreven, J. A. Montgomery, Jr., J. E. Peralta, F. Ogliaro, M. Bearpark, J. J. Heyd, E. Brothers, K. N. Kudin, V. N. Staroverov, T. Keith, R. Kobayashi, J. Normand, K. Raghavachari, A. Rendell, J. C. Burant, S. S. Iyengar, J. Tomasi, M. Cossi, N. Rega, J. M. Millam, M. Klene, J. E. Knox, J. B. Cross, V. Bakken, C. Adamo, J. Jaramillo, R. Gomperts, R. E. Stratmann, O. Yazyev, A. J. Austin, R. Cammi, C. Pomelli, J. W. Ochterski, R. L. Martin, K. Morokuma, V. G. Zakrzewski, G. A. Voth, P. Salvador, J. J. Dannenberg, S. Dapprich, A. D. Daniels, O. Farkas, J. B. Foresman, J. V. Ortiz, J. Cioslowski, and D. J. Fox, Gaussian, Inc., Wallingford CT, 2010.

**Table S18.** Calculated Geometry for [trans-NiF(2,3,5,6-C<sub>6</sub>F<sub>4</sub>)(PMe<sub>3</sub>)<sub>2</sub>]

Center Number	Atomic Number	Atomic Type	Coordinates (Angstroms)		
			X	Y	Z
1	6	0	0.416066	0.654293	-0.954560
2	6	0	1.797250	0.668513	-0.975531
3	6	0	2.515377	-0.000001	-0.000001
4	6	0	1.797242	-0.668514	0.975523
5	6	0	0.416057	-0.654291	0.954541
6	6	0	-0.336879	0.000001	-0.000012
7	9	0	2.427851	1.335302	-1.940599
8	9	0	2.427833	-1.335304	1.940596
9	9	0	-4.090432	0.000007	-0.000010
10	28	0	-2.268998	0.000004	-0.000013
11	15	0	-2.529723	-2.219516	-0.436460
12	9	0	-0.211064	1.344869	-1.931308
13	15	0	-2.529711	2.219520	0.436465
14	53	0	4.615859	-0.000005	0.000004
15	6	0	-3.494591	-3.009493	0.895699
16	1	0	-4.386057	-2.414395	1.062351
17	1	0	-3.773001	-4.027291	0.633702
18	1	0	-2.908800	-3.024544	1.809756
19	6	0	-3.566145	-2.452497	-1.920699
20	1	0	-3.853764	-3.493681	-2.043598
21	1	0	-4.450567	-1.834503	-1.809371
22	1	0	-3.025286	-2.128224	-2.804927
23	6	0	-1.120923	-3.354582	-0.695620
24	1	0	-1.466986	-4.362300	-0.911490
25	1	0	-0.512323	-3.005328	-1.524260
26	1	0	-0.501333	-3.377470	0.195141
27	6	0	-1.120905	3.354583	0.695601
28	1	0	-0.512283	3.005319	1.524221
29	1	0	-0.501338	3.377481	-0.195176
30	1	0	-1.466962	4.362298	0.911492
31	6	0	-3.494620	3.009517	-0.895652
32	1	0	-4.386084	2.414414	-1.062295
33	1	0	-3.773033	4.027308	-0.633626
34	1	0	-2.908852	3.024594	-1.809724
35	6	0	-3.566088	2.452473	1.920739
36	1	0	-3.025208	2.128171	2.804943
37	1	0	-3.853694	3.493657	2.043673
38	1	0	-4.450521	1.834491	1.809420
39	9	0	-0.211080	-1.344866	1.931286

**Table S19** Calculated Geometry for [trans-NiF(2,3,5,6-C<sub>6</sub>F<sub>4</sub>I)(PMe<sub>3</sub>)<sub>2</sub>] + (2,3,5,6-C<sub>6</sub>F<sub>4</sub>I)

Center Number	Atomic Number	Atomic Type	Coordinates (Angstroms)		
			X	Y	Z
1	6	0	3.625770	-0.820467	0.817517
2	6	0	5.007019	-0.837330	0.835521
3	6	0	5.725047	-0.000003	-0.000022
4	6	0	5.007017	0.837326	-0.835562
5	6	0	3.625768	0.820468	-0.817549
6	6	0	2.874906	0.000002	-0.000014
7	9	0	5.637031	-1.670430	1.660723
8	9	0	5.637027	1.670424	-1.660767
9	9	0	-0.886367	0.000008	0.000000
10	28	0	0.948922	0.000005	-0.000008
11	15	0	0.740002	2.036409	1.006441
12	9	0	2.995556	-1.679055	1.647039
13	15	0	0.739990	-2.036399	-1.006455
14	53	0	7.825247	-0.000007	-0.000029
15	6	0	-0.195383	3.189312	-0.055022
16	1	0	-1.121678	2.712140	-0.356286
17	1	0	-0.416430	4.115634	0.469234
18	1	0	0.384475	3.413815	-0.945118
19	6	0	-0.267057	1.918865	2.525176
20	1	0	-0.483497	2.904766	2.928997
21	1	0	-1.195367	1.409880	2.289483
22	1	0	0.263024	1.338871	3.274878
23	6	0	2.198267	3.006581	1.524769
24	1	0	1.894672	3.933523	2.004454
25	1	0	2.800361	2.429532	2.219906
26	1	0	2.809561	3.240844	0.659170
27	6	0	2.198250	-3.006571	-1.524797
28	1	0	2.800336	-2.429524	-2.219939
29	1	0	2.809551	-3.240834	-0.659203
30	1	0	1.894649	-3.933514	-2.004478
31	6	0	-0.195385	-3.189301	0.055018
32	1	0	-1.121678	-2.712129	0.356290
33	1	0	-0.416438	-4.115624	-0.469236
34	1	0	0.384481	-3.413804	0.945108
35	6	0	-0.267084	-1.918855	-2.525180
36	1	0	0.262992	-1.338862	-3.274888
37	1	0	-0.483530	-2.904756	-2.928998
38	1	0	-1.195391	-1.409867	-2.289478
39	9	0	2.995552	1.679058	-1.647068
40	9	0	-5.836364	-1.779675	1.539746
41	9	0	-8.503914	-1.770646	1.532150

42	6	0	-6.460433	-0.894002	0.773750
43	6	0	-7.841928	-0.902561	0.781178
44	53	0	-3.635346	0.000003	0.000015
45	6	0	-5.741444	-0.000001	0.000026
46	6	0	-8.535667	-0.000007	0.000040
47	6	0	-6.460445	0.893996	-0.773691
48	6	0	-7.841939	0.902550	-0.781105
49	9	0	-5.836387	1.779672	-1.539694
50	9	0	-8.503937	1.770633	-1.532070
51	9	0	-9.857779	-0.000009	0.000047

## References

1. J. Cosier and A. M. Glazer, *J. Applied Crystallogr.*, 1986, **19**, 105-107.
2. L. Palatinus and G. Chapuis, *J. Applied Crystallogr.*, 2007, **40**, 786-790
3. P. W. Betteridge, J. R. Carruthers, R. I. Cooper, K. Prout and D. J. Watkin, *J. Applied Crystallogr.*, 2003, **36**, 1487-1487.